Isotope Geochemistry

Chapter 7 The Continental Crust & Oceans

Radiogenic Isotope Geochemistry of the Continental Crust and the Oceans

7.1 Introduction

The continental crust is the most accessible part of the Earth and therefore certainly the part we know most about. That, however, is not to say that we know it well; there is still uncertainty about the overall composition, age, and evolution of the crust. This is to say that there is still much work left for future generations of earth scientists, and geochemists in particular. This is because the continental crust is remarkably complex tapestry of terranes with different histories. In the previous chapter we assumed that the crust has been created through time (rather than all at the beginning, as the core was). In this chapter we will review the evidence that this was indeed the case. Isotope geochemistry is a particularly powerful tool in unraveling crustal genesis, precisely because the crust has evolved and changed over time. The Earth has, of course, two kinds of crust: continental and oceanic. The continental crust is thick, low density, and persistent. The oceanic crust is thin, dense, and ephemeral, continually being created and destroyed such that its average age is only 60 million years. It consists almost entirely of mid-ocean ridge basalts and related intrusive rocks. It is compositionally and structurally simple in comparison to continental crust. In this chapter we will focus on continental crust, which, being thicker and more persistent, better qualifies and an important terrestrial reservoir.

Erosion products of the continents are carried to the oceans by rivers and winds. Hydrothermal systems at mid-ocean ridges and elsewhere also add radiogenic elements, most notably Sr, to seawater. This processes lead to isotopic variations in seawater in space and time. In the latter part of this chapter, we will see how radiogenic isotope ratios in seawater and sediments precipitated from seawater are used to trace the evolution of the Earth's surface through time as well to trace changing patterns of ocean circulation.

7.2 Growth of the Continental Crust Through Time

7.2.1 Mechanisms of Crustal Growth

There is unanimous agreement the crust has formed through magmatism: partial melting of the mantle followed by buoyant rise of those melts to the surface. There is less agreement on the details. Furthermore, the composition of the continental crust is problematic in the context of this hypothesis because it does not have the composition of a mantle-derived magma. This suggests that evolution of the crust is more complex than simple melt extraction from the mantle. We can identify a number of possible mechanisms that would result in the creation of new continental crust. Most of these mechanisms suffer from the problem that they result in a more mafic crust than that observed.

- *Accretion of oceanic crust and oceanic plateaus*. The oceanic crust is generally subducted and returned to the mantle. It might in unusual situations be thrust upon or under continental crust. Subsequent melting of the basalt could produce granite. Thick oceanic plateaus produced by mantle plumes such as Ontong-Java and Iceland would be subducted less readily than normal oceanic crust. Their isotopic composition would be less depleted.
- *Underplating*. Because of the low density of the continental crust, magmas have difficulty rising through it and may become trapped at the crust mantle boundary. This produces new basaltic lower crust, which upon remelting would produce a granitic upper crust.
- *Continental volcanism*. For example, flood basalts have occasionally been erupted in tremendous volumes. Volcanism and underplating may occur simultaneously.

• *Subduction-related volcanism.* Volcanism is usually present along active continental margins. Most of the magma is of mantle derivation. Accretion of intra-oceanic island arcs to continents is a closely related mechanism.

It is clear that at present, and almost certainly throughout the Phanerozoic, the last mechanism has produced the greatest additions to continental crust. It is tempting to assume this has been the case throughout geologic time, but this has not been demonstrated unequivocally. Because subduction zones appear to play such a key role in the evolution of the crust and mantle, we will discuss them in more detail in a subsequent section. In all the above-mentioned mechanisms, there must be some additional mechanism by which the crust loses a mafic component. The most probable is lower crustal foundering: the lower crust under some circumstances become so dense that it sinks into the mantle. In addition, weathering and erosion tend to remove Mg in preference to Si and Al. Rivers then carry Mg to the ocean where hydrothermal activity transfers it into the oceanic crust.

7.2.2 The Hadean Eon and the Earliest Continental Crust

The Hadean eon is defined as the time of Earth's formation and preceding the geologic record. The oldest surviving continental crust is the 3.92 Ga Acasta gneiss in Canada's Northwest Territory, and thus marks beginning of the geologic record and the end of the Hadean eon (defined as the time before the oldest rocks). One zircon from the Acasta gneisses has a 4.20±0.06 Ga core surrounded by a rim with an age of 3.8 to 3.9 Ga (Iizuka et al., 2006) indicating these gneisses formed from even older, Hadean crustal protoliths. Even older zircon cores, with ages of up to 4.4. Ga, have been found in mid- to late-Archean quartzite (metamorphosed sandstone) from the Jack Hills of western Australia. The Acasta and Jack Hills zircons are the only known survivors of the Earth's Hadean eon. As we will see, however, isotope ratios of rocks from the subsequent Archean eon provide insights into this earliest part of Earth's history.

7.2.2.1 Evidence of a Late Accretionary Veneer?

As we found in Chapter 5, ^{182}Hf (half-life 9 Ma) was present in the early Solar System and the silicate Earth's $^{182}W/^{184}W$ is about 2 epsilon units higher than chondrites. The difference reflects sequestration of W in the Earth's core (or, more likely, the cores of the planetary embryos that accreted to form the Earth) before ^{182}Hf completely decayed, leaving the silicate Earth and Moon enriched in ^{182}W. Subsequently, increased precision has led to the discovery of small variations in ε_W in Archean rocks. Willbold et al. (2011) reported an average ε_W of +0.13±0.04 (2σ) for 7 samples of 3.8 Ga Isua (S.W. Greenland) including gneisses, metabasalts and metasediments (individual samples were identical within analytical error). The positive values imply the source of these rocks had a higher Hf/W ratio than modern Earth materials. How can we explain this? The hint is that the silicate Earth is richer in siderophile elements such as W, Re, and Os than one would expect from equilibrium partitioning between a metal core and silicate mantle (see section 2.7). A long-standing hypothesis to explain this is addition of a 'late veneer' of chondritic material that accreted to the Earth after final segregation of the core in the Moon-forming giant impact (Chou, 1978; Wänke et al, 1984). A later veneer is consistent with the cratering history of the Moon, which culminates in a 'late heavy bombardment' at about 3.9 Ga as well as with computer simulations of planetary accretion. An amount of chondritic material equaling less than 1% of the mass of Earth would explain the high siderophile abundances in the silicate Earth. If this late veneer were undifferentiated chondritic material it would have ε_W of -2 (Figure 5.13), so adding it would decrease the ε_W of the Earth. If the Earth today has ε_W of 0, it must have had a higher value before the addition of the late accretionary veneer. This is just what Willbold et al. (2011) proposed, namely that the Isua samples retain a memory of the Earth's ε_W before addition of the late accretionary veneer. The decline of Earth's ε_W from +0.13 to 0 is consistent with addition of just under 0.5% by mass of chondritic material. The data do not directly constrain the timing of the addition, but are most easily explained if the addition occurred after ^{182}Hf was effectively extinct, or more than ~50 million years after the start of the solar system. All the analyzed rocks display excesses in ^{142}Nd that, as we discuss in

the next section, implying they formed from precursor material that had differentiated from the primitive mantle within ~200 million years or less of the start of the solar system.

The following year, Touboul et al., (2012) reported ε_W averaging +0.15±0.05 in 2.8 billion year old komatiites (which are ultramafic lava flows) from Kostomucksha in the Karelia region the Baltic Shield of northeastern Russia. Several interpretations are possible: that metal separated from the mantle source region of these lavas earlier than the rest of the Earth's mantle; that silicate differentiation of the mantle fractionated Hf/W ratios subsequent to core formation; or that the lavas are derived from a part of the mantle into which the late veneer has not been mixed. Touboul et al. also reported that 3.5 billion year old komatiites from Komati, South Africa, have normal tungsten isotopic composition. Willbold et al. (2013) reported ε_W values comparable to those found in rocks from the Isua supracrustal belt in the 3.92 Ga Acasta gneisses of the Northwest Territories of Canada and Touboul et al. (2013) reported that the 3.8 Ga Nuvvuaggittuq supracrustals of Labrador have ε_W of +0.15, similar to the Isua supracrustals and Kostomucksha komatiites. They also found that much younger 2.4 Ga Vetreny komatiites, located to the southeast of the Karelia region in Russia have slight ^{182}W excesses, averaging ε_w of +6.2±4.5 ppm (2σ, n = 5). In contrast, they found that the 3.3. Ga Barberton komatiites of South Africa have tungsten isotopic compositions similar to the modern Earth (i.e., $\varepsilon_W \approx 0$). As may be seen in Figure 5.13, these variations are small compared to those observed in extraterrestrial materials.

Thus the silicate Earth appears to have had a heterogeneous tungsten isotopic composition in the Archean, perhaps because convection had not yet succeeded in mixing the late accretionary veneer into the mantle or to fully homogenize the mantle following crystallization of a magma ocean. The uniform ε_W in the 3 early Archean localities, Isua, Acasta, and Nuvvuaggittuq, however, is consistent with the idea that mantle that had an initially homogeneous ε_W of about +0.15 and that ε_W subsequently decreased to 0 as a late veneer of chondritic material was slowly mixed into the mantle. Subsequent convection apparently homogenized the mantle such that only a hint of the initial higher ε_W remained by the early Proterozoic and no trace of that remains today as all modern mantle-derived rocks have uniform ε_W.

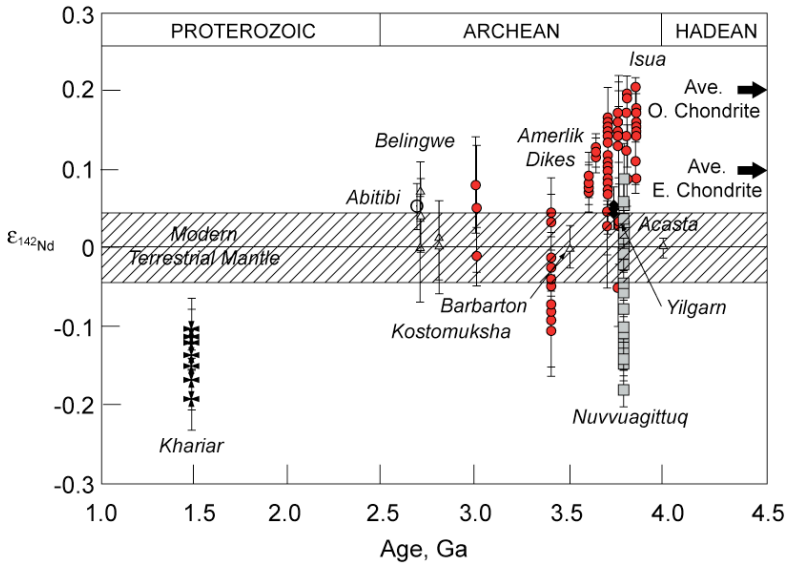

Figure 7.1. $^{142}Nd/^{144}Nd$ (expressed in epsilon units from a terrestrial standard) as a function of age in terrestrial samples. Red circles are from Greenland, grey squares from Labrador, black diamonds from western Australia, and crosses from Khariar, India, black circle from Theo's Flow, Canada. Modified from Bennett et al. (2007) and Rizo et al. (2012) with additional data.

7.2.2.2 ^{142}Nd Evidence of Hadean Crust Formation

In addition to the Acasta gneisses, early Archean crust of approximately 3.7 Ga older has been found in Greenland, Labrador, western Australia, and India. The total volume of this crust, however, is quite small. This raises some profound questions: how and when did the earliest crust form? Did only a small volume form initially, or did a much larger volume form, with only a small fraction of that surviving to the present?

$^{142}Nd/^{144}Nd$ ratios along with $^{176}Hf/^{177}Hf$ and $^{143}Nd/^{144}Nd$ are beginning to provide fairly clear evidence that differentiation of the Earth

began early (Figure 7.1). As we found in Chapter 5, modern terrestrial samples have $^{142}Nd/^{144}Nd$ that is about 20 ppm, or 0.2 epsilon units, higher than chondritic. However, samples from the early Archean Amitsoq Complex of West Greenland have $^{142}Nd/^{144}Nd$ that is up to an additional 20 ppm higher than that (Caro et al., 2003, Boyet and Carlson, 2005, 2006; Bennett et al., 2007, Rizo et al. 2013). $^{142}Nd/^{144}Nd$ excess of 5 ppm were also found in two 3.7 Ga tonalites* from the Yilgarn block western Australia (Bennett et al., 2007). The $^{142}Nd/^{144}Nd$ excesses indicate that these early crustal rocks were derived from a mantle reservoir having a Sm/Nd ratio higher than chondritic and higher than modern bulk silicate (observable) Earth. High Sm/Nd ratios are indicative of trace element depletion, indicating these rocks were derived from mantle that had experienced even earlier episodes of crust creation. An early incompatible element-enriched crust that formed either by fractional crystallization of a primordial magma ocean or by partial melting of the mantle, would leave part of the mantle incompatible element-depleted. Early Archean crust formed by subsequent melt extraction from that depleted mantle would have high $^{142}Nd/^{144}Nd/$. Thus some of the oldest rocks on Earth suggest crust formation began even earlier – well before 4.0 Ga and arguably before 4.4 Ga. On this point there is no debate. The crucial question, and one that is debated, is how much?

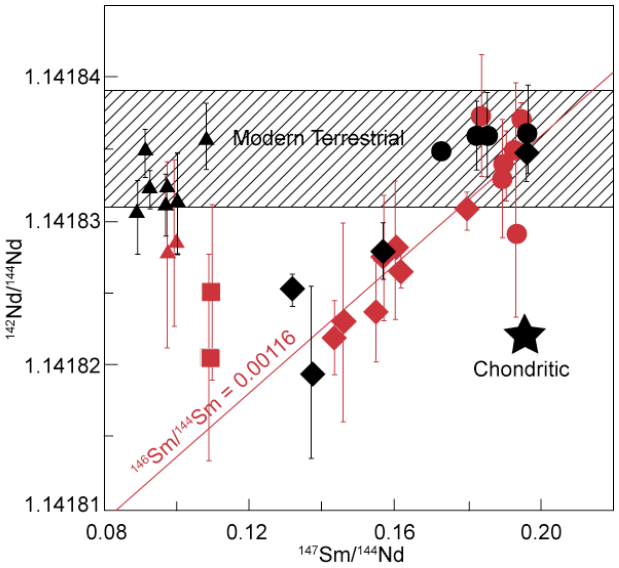

Figure 7.2. $^{142}Nd/^{144}Nd$ vs. $^{147}Sm/^{144}Nd$ for rocks from the Nuvvaugittuq Belt of northwestern Labrador. The slope of the line corresponds to a $^{146}Sm/^{144}Nd$ ratio of 0.00116. If this line is interpreted as an isochron, it implies a formation age of 4.36 Ga. Triangles: felsic gneisses, diamonds, cummingtonite amphibolite, circles: hornblende amphibolites. Red symbols from O'Neil et al. (2008); black symbols from Roth et al. (2013). Modified from O'Neil et al. (2008) and Roth et al. (2013).

A particularly interesting twist to this was reported by O'Neil et al. (2008). They found negative ε_{142Nd} values in amphibolites from the Nuvvaugittuq Belt of northwestern Labrador and this has recently been confirmed by additional analyses of O'Neil et al. (2012) and Roth et al. (2013). There is a strong correlation between $^{142}Nd/^{144}Nd$ and $^{147}Sm/^{144}Nd$ in a subset of rocks from the area, cummingtonite amphibolites (Figure 7.2). As we found in Chapter 5, when an extinct radionuclide is involved, the slope of the line on plots such as this is proportional to the parent isotope ratio, in this case $^{146}Sm/^{144}Sm$, at the time the rocks formed. Using both the data from O'Neil et al. and Roth et al., the slope in the case for the cummingtonite amphibolites corresponds to $^{146}Sm/^{144}Sm = 0.00116$. Using a ^{147}Sm half-life of 68 Ma and the solar system initial $^{146}Sm/^{144}Nd$ of 0.0094, the apparent age is 4.36 Ga. Other suites of rocks from the region yield $^{142}Nd/^{144}Nd$–$^{147}Sm/^{144}Nd$ pseudo-isochrons corresponding to ages ranging from 4.31 to 4.41 Ga (O'Neil et al., 2012). However, a $^{147}Sm/^{144}Nd$–$^{143}Nd/^{144}Nd$ isochron for the cummingtonite amphibolites gives an age of only 3.89 Ga with considerable uncertainty and other suites in the area give even younger ages. There are no zircons in the mafic rocks, but crystallization age of zircons in felsic rocks as well as detrital zircons in metasediments give ages that range from 3.75 to 3.78 Ga, which is likely the maximum age of the Nuvvaugittuq supracrustal belt (Cates, 2013).

* In brief, a *tonalite* is an alkali-poor, quartz-rich granite.

An alternative interpretation is that the Nuvvaugittuq $^{142}Nd/^{144}Nd$–$^{147}Sm/^{144}Nd$ correlations are mixing lines resulting from assimilation of early crust by a much later basaltic magma rising from the mantle. Modeling done by Cates et al. (2013) suggests this assimilated crust could have formed at 4.5 Ga, and that metamorphism of the amphibolites (which they speculate were originally pyroclastic rocks) formed around 3.8 Ga, resulted in decoupling of the $^{142}Nd/^{144}Nd$ and $^{143}Nd/^{144}Nd$ ages. While the amphibolite is much younger (3.8-4.0 Ga) in this interpretation, the $^{142}Nd/^{144}Nd$– $^{147}Sm/^{144}Nd$ correlation nevertheless provides evidence of an early-formed incompatible element-enriched crust with low Sm/Nd.

Rizo et al. (2011) subsequently reported ^{142}Nd deficits in the 3.4 Ga mafic Amerlik dikes, which intrude the early Archean Isua supracrustals and surrounding gneisses. They argue these magmas were derived from a low Sm/Nd reservoir that formed before 4.47 Ga either as a result of crystallization of a magma ocean or an early mafic protocrust.

The largest $^{142}Nd/^{144}Nd$ anomalies are found in the earliest Archean rocks. Variations in $^{142}Nd/^{144}Nd$ appear to decline through the Archean, and most rocks younger than 3.5 Ga have $\varepsilon_{^{142}Nd}$ whose errors overlap the range of the modern terrestrial mantle ($\varepsilon_{^{142}Nd} = 0\pm0.05$). One exception is Theo's flow, a komatiitic lava flow from the 2.7 Ga Abitibi belt in Quebec that has $^{142}Nd/^{144}Nd$ ratios ($\varepsilon_{^{142}Nd} = 0.07\pm0.03$) barely outside the modern mantle range (Debaille et al., 2013). Again, this positive $\varepsilon_{^{142}Nd}$ is the signature of mantle depleted in Nd relative to Sm by melting extraction in the first 100 Ma or so of Earth history, implying that remnants of this early depleted mantle persisted at least locally through much of the Archean. Debaille et al. (2013) point out that this is surprising since we would expect convective mixing to scale with heat production, which decreases exponentially with time. They suggest the persistence of heterogeneity implies a convective style that lacked subduction and plate tectonics and that was less efficient at mixing out mantle heterogeneity in the Archean. A variety of studies carried out with increasing precision have found that the modern mantle has a homogeneous $^{142}Nd/^{144}Nd$ (e.g., Jackson and Carlson, 2012), implying these heterogeneities were eventually erased.

The only case of ^{142}Nd anomalies in post-Archean rocks are the 1.48 Ga Khariar nepheline syenites from southeastern India, which have $\varepsilon_{^{142}Nd}$ as low as -0.13. Upadhyay et al. (2009) interpret these igneous rocks have having sampled a very ancient incompatible element-enriched reservoir that survived in the lithospheric mantle beneath the Bastar craton of India until 1.5 Ga. These data suggest that some parts of the mantle managed to avoid mixing processes that have homogenized isotopic and chemical heterogeneities that were present in the early mantle. That some heterogeneity survived for 3 billion years may be less surprising than the opposite observation: nearly all initial heterogeneity in the Earth's mantle has be eliminated by mixing. The Khariar syenites intruded into the Archean Bastar (or Bhandara) craton that include 3.5-Ga-old gneisses. Upadhyay et al. (2009) suggest that the Khariar syenites were derived from the lithospheric root beneath the ancient Bastar craton. Because the lithosphere does not experience convective mixing, ancient chemical and isotopic heterogeneity can survive. The Khariar results are presently somewhat controversial. As analytical precision improves, however, we may see additional examples of rocks with resolvable $^{142}Nd/^{144}Nd$ anomalies will be found, particularly in mid- to late Archean rocks.

Could the Archean $^{142}Nd/^{144}Nd$ heterogeneity, like that of $^{182}W/^{184}W$, be due to a late accretionary veneer? The answer is no. First, the difference in $^{142}Nd/^{144}Nd$ between the silicate Earth and chondrites is more than an order of magnitude smaller than for $^{182}W/^{184}W$. Second, the mantle is richer in Nd that are chondrites, while chondrites have 5 to 6 times greater W concentrations than does the mantle. Thus small a small addition of chondritic material affects the mantle's $^{182}W/^{184}W$, it has virtually no effect on its $^{142}Nd/^{144}Nd$.

7.2.2.3 Evidence of Hadean Crust from Zircons and ε_{Hf}

A few tiny detrital (that is, eroded from their original rocks and deposited in sediments) zircon crystals are all that remain of Hadean crustal rocks that once must have existed in Australia. The Jack Hills zircons occur in a metasedimentary conglomerate thought to be about 3 billion years old. The metasediments are surround by the Narryer gneisses (3.65- 3.3 Ga), which were intruded by granites at

2.65 Ga. The majority of zircon crystals are about 3.6-3.8 billion years old, but a small fraction are older than 4 billion years and the oldest date is 4.4 billion years (Figure 3.10). Despite the extremely small volume of this material, new micro-analytical techniques are providing a wealth of information on crust from which these crystals were eroded. The zircons have complex histories, and the very old ages were only discovered by analyzing individual zones with the ion microprobe (Froude et al., 1983; Compston and Pidgeon, 1986). More recently, it has become possible to determine Pb-Pb ages using laser ablation multi-collector inductively coupled plasma mass spectrometry (LA-MC-ICP-MS). This technique can also determine other isotope ratios and elemental abundances on regions as small as 50 μm in diameter. Hf is strongly concentrated in zircon so that Lu/Hf ratios are quite low. Consequently, initial Hf isotopic compositions are quite readily determined. Several groups had studied the Hf isotopic compositions of the zircons. However, interpretation is difficult because the zircons are often zoned with overgrowths as young as 3.3 Ga (Harrison et al., 2005). Blichert-Toft and Albarede (2008) determined both Pb-Pb ages and Hf isotopic compositions by bulk analysis using MC-ICP-MS. They found a nearly gaussian distribution of ages with a mode of about 4.1 Ga. Initial ε_{Hf} calculated for this time show range of values, with a mode of about -3. The negative values imply the zircons formed in rocks derived from an older incompatible element-enriched precursor. The problem with bulk analyses of zircons having complex histories is that it integrates diverse age and Hf isotope ratio in a single analysis, which can produce mixtures that are at best impossible to deconvolve.

Kemp et al. (2010) simultaneously determined both Hf isotope compositions and Pb-Pb ages on the Jack Hills detrital zircons as well as from the surrounding Narryer gneisses and intrusive granites. The new results reveal a much simpler picture of early crustal evolution than earlier studies. The data scatter about a relatively simple ε_{Hf} evolutionary path of increasingly negative ε_{Hf} with time (Figure 7.3), in contrast to the much greater scatter of earlier data. Recall that in a plot such as this of an isotope ratio vs. time, slopes are proportional to the parent-daughter ratio. The slope of the least disturbed detrital Jack Hills zircons corresponds to a $^{176}Lu/^{177}Hf$ ratio of about 0.019 and

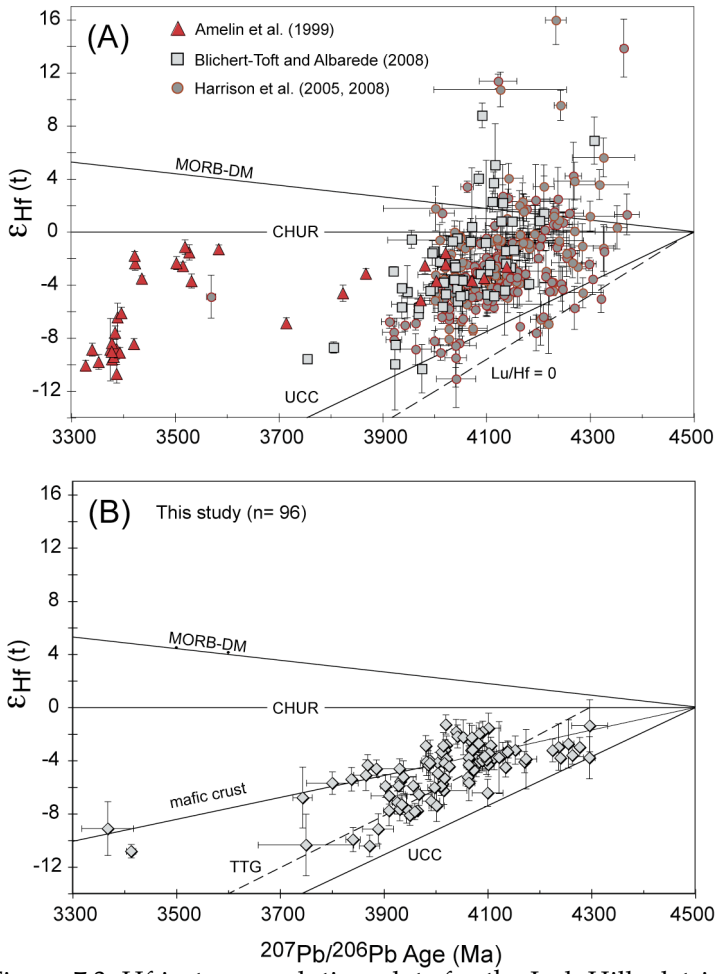

Figure 7.3. Hf isotope evolution plots for the Jack Hills detrital zircons comparing (a) previously published datasets with (b) data obtained during by Kemp et al. (2010). The isotope trajectories of upper continental crust), mafic crust and tonalite-tronjhemite granite suites (TTG) (formed at 4.3 Ga with $^{176}Lu/^{177}Hf$ = 0.005, Blichert-Toft and Albarède, 2008) are shown for reference as is a depleted mantle-MORB evolution curve (MORB-DM). From Kemp et al. (2010).

project back to $\varepsilon_{Hf} = 0$ at 4.46±0.12 Ga. This Lu/Hf ratio is typical of mafic (i.e., basaltic) rocks. In Kemp et al.'s (2010) interpretation, the zircons were derived from granitic rocks produced by partial melting of an enriched, dominantly mafic protolith that was extracted from primordial mantle at 4.4–4.5 Ga. The lowest ε_{Hf} in zircons from younger meta-igneous Narryer gneisses plot near an extension of the ε_{Hf} – time array defined by the Hadean detrital zircons (Figure 7.4). From this, Kemp et al. argue that Hadean crust may have contributed substantially to the younger Archean magma. Vervoort et al. (2013) caution, however, that ancient Pb loss in these old complex zircons can produce younger apparent ages that are unrelated to crustal reworking. They further argue that the depleted mantle evolution curve (shown in Figures 7.3 and 7.4) for Hf is poorly constrained and may not diverge from CHUR until nearly 3.8 Ga. The implication of this is that large-scale crustal formation may have not begun prior to 3.8 Ga.

Remarkably, the Jack Hills zircons plot along the same evolutionary path displayed by zircons from Apollo 14 lunar breccias (Taylor et al., 2009). From this Kemp et al. speculate that the mafic protolith may have formed during the solidification of a terrestrial magma ocean analogous to the lunar one.

As Figure 7.4 shows, data from early Archean rocks from Greenland, Acasta, and the Baltic plot along trajectories with slopes implying slightly higher $^{176}Lu/^{177}Hf$ that the Jack Hills data and intersecting the CHUR or depleted mantle evolution curves somewhat later, but nevertheless before 4.0 Ga. That would in turn imply that these rocks may also have been derived from Hadean protoliths. The implied Lu/Hf higher relative to modern upper continental crust suggests early Archean crust may have been more mafic. Indeed, it is likely thick felsic crust could not have survived long in the Archean because much higher radioactive heat production would have caused it to melt.

There is also some Pb isotope evidence that differentiation of the silicate Earth began very early. Figure 7.5 shows initial Pb isotope ratios from sulfide ores associated with submarine volcanic rocks that erupted in the Abitibi Belt of Canada around 2.7 Ga ago. The data plot virtually along the 2.7 Ga Geo-

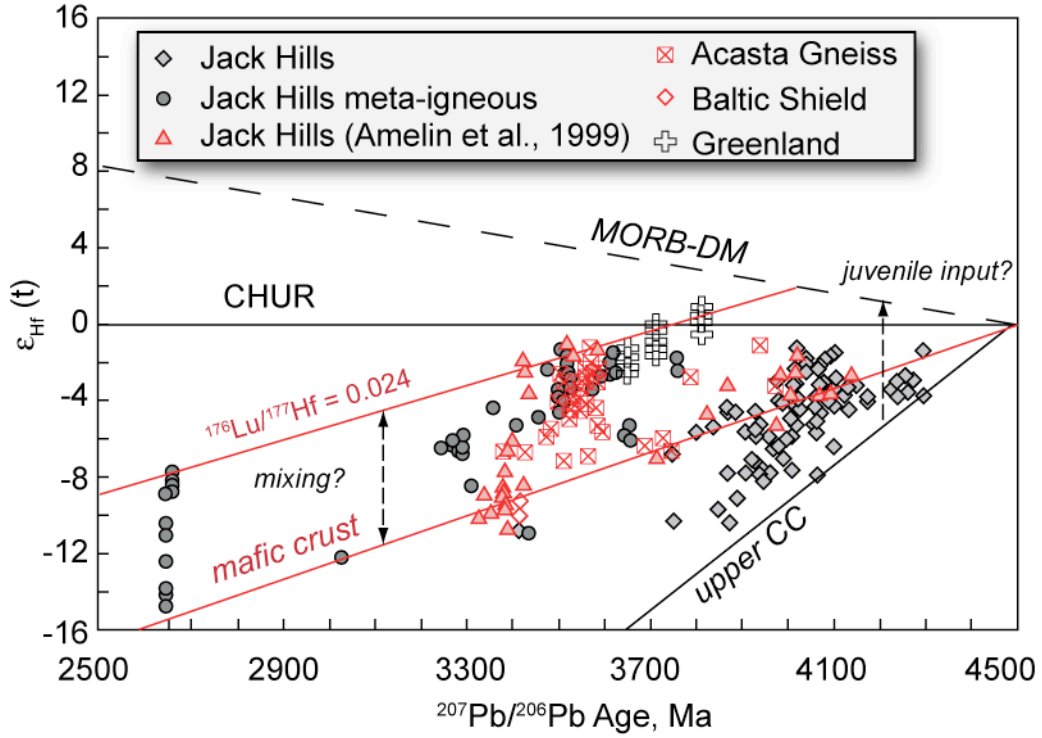

Figure 7.4. Hf isotope composition of zircons from the Jack Hills meta-igneous rocks in comparison to data from the detrital Jack Hills zircons, Greenland, the Acasta Gneisses, and the Baltic Shield. From Kemp et al. (2010).

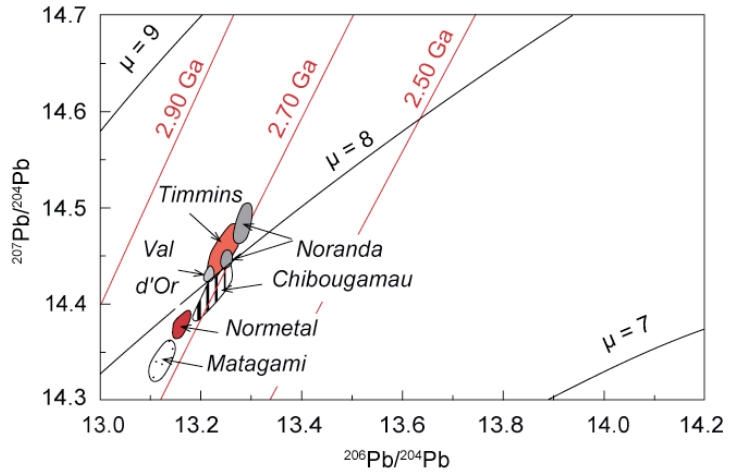

Figure 7.5. $^{207}Pb/^{204}Pb$–$^{206}Pb/^{204}Pb$ plot showing Pb isotopic fields volcanogenic massive sulfide deposits from the Abitibi greenstone belt. Also shown are single-stage Pb growth curves corresponding to μ values of 7, 8, and 9 and geochrons at 2.5, 2.7, and 2.9 Ga assuming an age for the Earth of 4.52 Ga. From Vervoort, et al. (1994).

chron (the Geochron as it was 2.7 Ga ago). The most straightforward interpretation of this data is that it reflects heterogeneity in the mantle that dates from the time the Earth formed, or shortly thereafter.

We may summarize by saying that there is now clear evidence from geochronology and from $^{176}Hf/^{177}Hf$ and $^{142}Nd/^{144}Nd$ for the existence of Hadean crust but the question of the volume of that crust remains the subject of vigorous debate, because none of this crust has survived. Reworking of this Hadean crust may have given rise to some of the earliest Archean rocks. Thus, we can conclude that the process of crust formation began very early in Earth's history, but certainly did not end in Hadean/Early Archean time.

7.2.3 Subsequent Growth of the Crust

If the crust has grown through time, at what rate and by what processes has it done so? We listed possible mechanisms at the start of the Chapter; all undoubtedly operate, but which is dominant? While there is as yet no definitive answer to this question, it certainly has been given considerable study. Perhaps the first quantitative attempt to determine continental evolution rate was by Hurley and others (1962). They compiled radiometric ages (mainly Rb-Sr) of rocks in the North American continent to produce a map that looked similar to that shown in Figure 7.6. Hurley et al. recognized that age provinces in Figure 7.6 could be produced by either tectonic reworking (melting, metamorphism, etc.), of preexisting crust or new additions to crust. They also recognized they could distinguish reworked crust from new crust by initial Sr isotope ratios. They argued that because the crust has a higher Rb/Sr ratio than the mantle, new additions to crust should have lower initial $^{87}Sr/^{86}Sr$ ratios than material produced by reworking old crust. From consideration of both age and initial isotopic composition, they argued that the

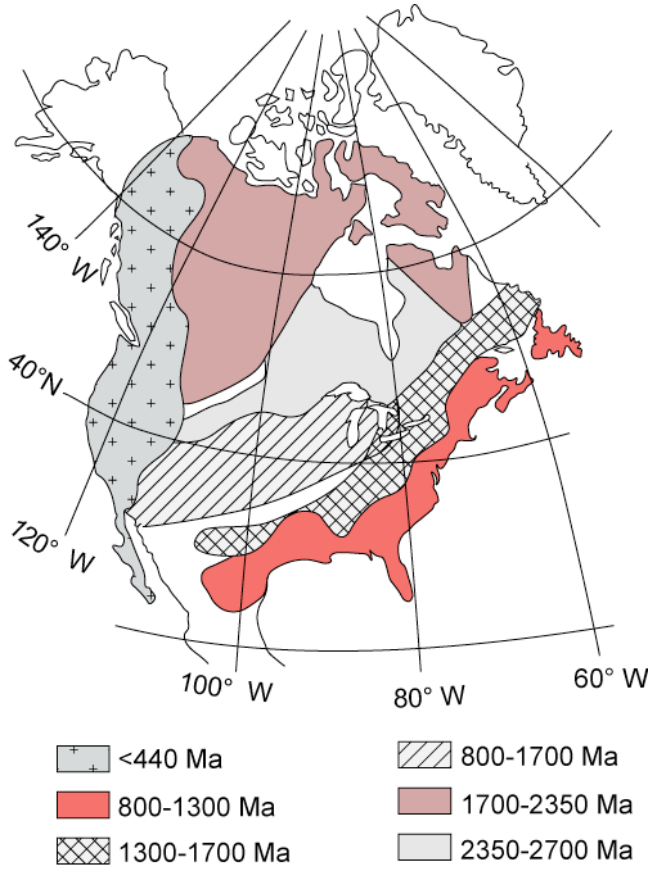

Figure 7.6. Age provinces of the North American continent (after Hurley and Rand, 1969).

crust had grown at a more or less steady rate through geological time.

The Rb-Sr system is particularly subject to resetting during metamorphism, so this is certainly not the best geochronological system to determine the times at which new magmas were added to the continental crust. Condie (1995) and subsequently Condie and Aster (2010) compiled zircon ages, which are shown in Figure 7.7. There are several important results from this study. First, zircon ages are concentrated at 2700, 1870, 1000, 600, and 300 Ma, with the number of zircon ages in these peaks decreasing through time (there are sufficient numbers of age determinations, ~40,000, to guarantee that these peaks are not random artifacts). If these ages represent new additions to crust, then overall, crustal grow rates have slowed through time. A generally decreasing rate is what we might expect since the Earth is cooling and heat, both initial and radiogenic heat, is the source of energy for magmatism and tectonic activity. The peaks in the age histograms appear to coincide with supercontinent formation and the minima with supercontinent breakup.

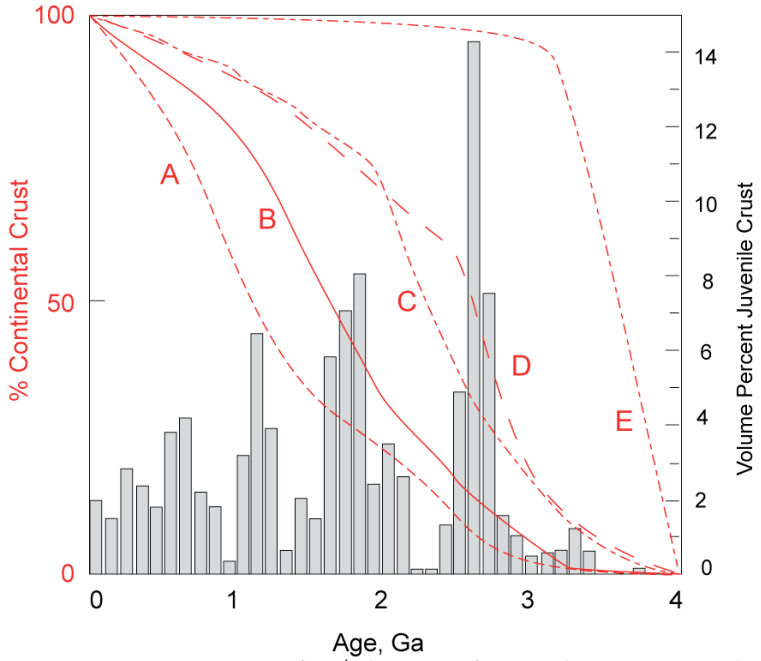

Figure 7.7. Histogram of U/Pb ages of juvenile igneous rocks (from Condie and Aster, 2010) compared with curves representing different models for changing volumes of stable continental crust through time. Curve A is Hurley and Rand (1969), B is based on Nd isotopes in shales (Allegre and Rousseau, 1984), C from Pb isotope modeling (Kramers and Tolstikhin, 1997) and D from Taylor and McLennan (1995) and E from Armstrong (1981). After Hawkesworth and Kemp (2006).

Figure 7.7 also shows a variety of estimates of how crustal growth rates have varied through time, which are framed by the extreme estimates by Hurley and Rand (1969) and Armstrong (1981b). As discussed above, the Hurley estimate was based on Rb-Sr geochronology and very likely overestimates the amount of young crust. Armstrong argued for a steady-state crustal mass. In his model the continental crust reached more or less its present mass in the early Archean and its mass has remained approximately constant because new additions to crust have been balanced by losses as a result of erosion, sedimentation, and subduction. At least at present, this seems to be the case. Scholl and von Huene (2009) estimate the amount of continental crust being transported into the mantle (a combination of sediment subduction and subduction erosion) at 3.2 km^3/yr* and the rate of additions to crust through subduction zone magmatism at 2.8-3.0 km^3/yr; in other words crustal production and destruction are currently roughly in balance. The distribution of zircon crystallization ages shown in Figure 7.7 cannot rule out Armstrong's hypothesis because zircons can only record the ages of crust that was melted, in view of the comparatively large amount of surviving late Archean crust, the lack of surviving early Archean crust is surprising if Armstrong's hypothesis is correct. While the full crustal mass may not have been established by 4 Ga, Armstrong's steady-state model could survive in modi-

Nd was thelessed in

* Units of km^3/yr are sometimes called Armstrong Units after Dick Armstrong and abbreviated (with tongue in cheek) as AU.

fied form, however, as Hawkesworth et al. (2010) suggest that the present continental crust mass was established by 2–3 Ga.

Do the zircon crystallization ages shown in Figure 7.7 record new additions to crust or something else? Condie and Aster (2010) interpret the zircon age histogram as "probably related chiefly to preservation of juvenile crust in orogens during supercontinent assembly." Hawkesworth et al. (2010) concur, suggesting that the peaks are artifacts of preservation marking the times of supercontinent formation. Hawkesworth et al. (2010) point out that magmatism associated with continental collisions (such as India and Asia) is dominated by remelting of older crust and granitic magmas, which are what dominate the upper continental crust). They also suggest that detritus, including detrital zircons, eroded from the collisional orogenic belts in the cores of supercontinents are more likely to be preserved than detritus from subduction zone volcanism. Thus, they argue that, "that the record of magmatic ages is likely to be dominated by periods when supercontinents assembled, not because this is a major phase of crust generation but because it provides a setting for the selective preservation of crust. The preservation potential, particularly for crystallization ages of zircons, is greater for late-stage collisional events as the supercontinents come together, rather than for subduction- and extension-related magmatism", whereas it is the latter processes that predominantly create new continental crust. The record shown in Figure 7.7 is that much of that initially created crust does not long survive. Initial Nd and Hf isotope ratios and model ages provide approaches that can get around issue of preferential preservation, and we explore them next.

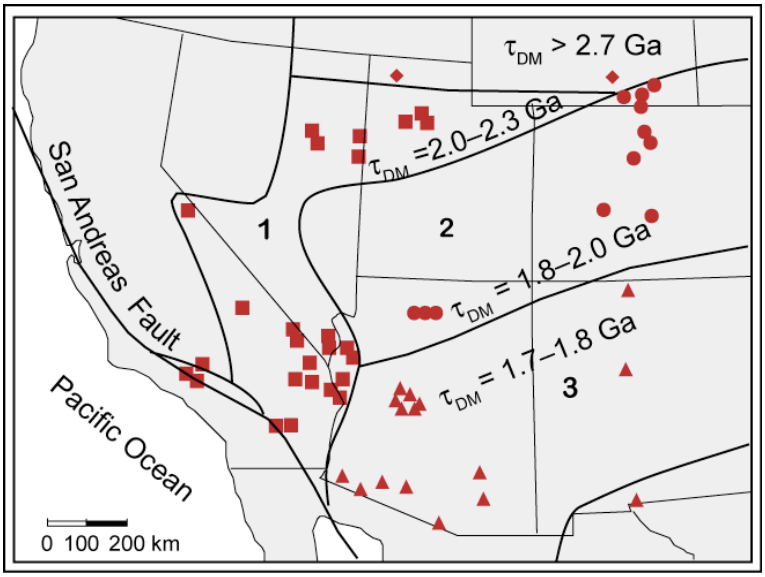

Figure 7.8. Isotopic provinces, based on crustal residence times (T_{DM}) of the Western U.S. (Bennett and DePaolo, 1987).

7.2.4 Nd and Hf Isotopic Approaches to Crustal Evolution

Nd isotope systematics provides a wonderful tool for examining the evolution of the continental crust. We have already discussed the concept of the Nd model ages, or crustal residence times (section 2.5.1). Hf model ages can be calculated in an exactly analogous manner, although one must be cautious since Lu and Hf are relatively easily fractionated within the crust, unlike Sm and Nd. Here we will see how model ages can be used to infer when crustal material was first derived from the mantle. We begin by examining the work of Bennett and DePaolo in the Western US.

Figure 7.8 is a map of the Western U.S. showing contours of crustal residence times (τ_{DM}). The data define 3 distinct provinces and suggest the existence of several others. There is a general similarity to Hurley's map, but the Nd work shows greater detail, and the ages are often older. Figure 7.9 shows the initial ε_{Nd} values of the granites from the three number provinces plotted as a function of crystallization age. Only in province 3 do we find rocks, tholeiitic and calc-alkaline greenstones, whose crustal residence time is equal to their crystallization ages. In the other regions, the oldest rocks have initial ε_{Nd} values that plot below the depleted mantle evolution curve. This suggests they contain significant amounts of pre-existing crust. We should emphasize at this point that the crustal residence time gives the average crustal residence time of Nd in the material. Thus if a continental rock formed at 1.0 Ga contained Nd derived in equal proportions from the mantle and 2.0 Ga crust, its crustal residence time

would be 1.5 Ga. In each province there have been subsequent episodes of magmatism, but in those subsequent episodes there have been no new additions of crust (they plot along the same evolutionary array as the older material in the province).

All three provinces apparently formed between 1.8 and 1.65 Ga, though rocks from province 1 may be slightly older. A scenario suggested by DePaolo that is consistent with the observations is successive accretion or growth of island arcs to the preexisting Archean craton to the north. The earliest formed arcs, or at least those closest to the craton received a substantial component of older crust from the craton. This could have occurred through erosion and subduction, or, if the arc was built directly on the continent, through assimilation of crust. As new Proterozoic crust was built outward from the continent, it screened subsequent arcs from the contribution of material from the Archean crust. A similar effect has been observed in the Proterozoic provinces of Canada.

The Paleozoic Lachlan Fold Belt of southeastern Australia provides another interesting case study. Chappell and White (1974) divided the granites of this region into I- and S-types, introducing what has become a widely used terminology. The I- (for igneous) type are metaluminous $(((Ca+Na+K)/Al)_{atomic}$ >1) to weakly peraluminous, with high CaO and Ca/ Na, and usually contains hornblende and are thought to be derived by melting of a meta-igneous protolith. The S (for sedimentary) types are strongly peraluminous $(((Ca+Na+K)/Al)_{atomic}$<1), typically cordierite- bearing and have generally lower abundances of seawater soluble elements (Na, Ca and Sr), and are through to be derived by melting of a metasedimentary protolith. Despite the difference in origin, the trace element compositions are similar and they define a single overlapping array on an ε_{Nd}-$^{87}Sr/^{86}Sr$ diagram. As a result, in contrast to the Southwestern U.S. discussed above, it has not been possible to resolve whether the low ε_{Nd} of some of the I-type granites reflect contamination by melts of metasediments or derivation from meta-igneous protoliths of different crustal residence ages.

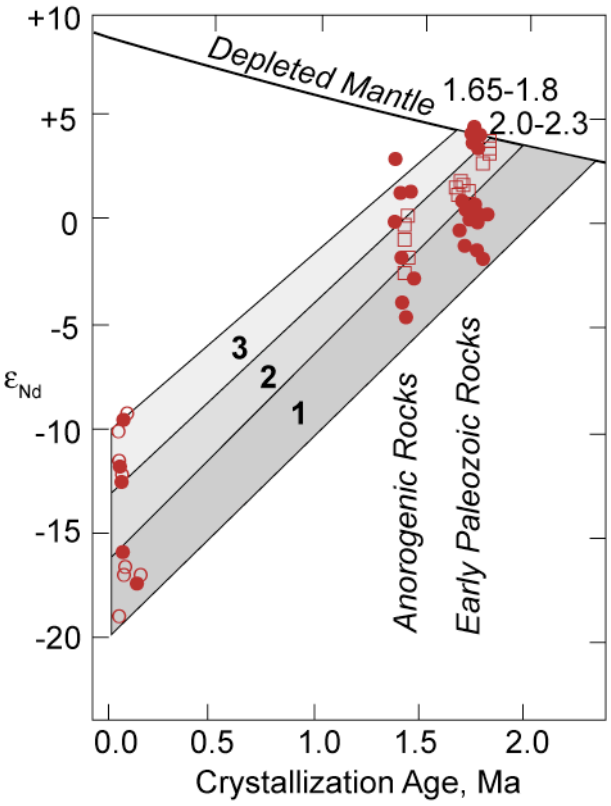

Figure 7.9. ε_{Nd} (initial) as a function of crystallization age of Western U.S. Groupings 1 2, and 3 refer to provinces shown in Figure 7.8.

Hawkesworth and Kemp (2006) combined LA-MS-ICP-MS to determine ages and Hf isotopic compositions of zircons with ion microprobe analysis to determine O isotope ratios on 2 suites of I-type granites. As we'll learn in Chapter 9, $\delta^{18}O$ values of the mantle and purely mantle-derived magmas are uniform at values around +5 to +6. Higher values indicate that rocks have interacted with water on the surface or within the crust. Both suites show a range of $\delta^{18}O$ values extending down to mantle-like values. In one suite, the O-ε_{Hf} relationship suggested mixing between a juvenile mantle magma and melts of a sedimentary protolith; in the other suite, it suggested mixing between mafic crust that has evolved to lower ε_{Hf} and a sedimentary protolith (Figure 7.10). Hawkesworth and Kemp (2006) also analyzed detrital zircons from the metasediments of the Lachlan Fold Belt. The crystallization age spectra of the detrital zircons are dominated by peaks at 450–600 Ma and 0.9–1.2 Ga. Hf model ages of zircons, which were calculated assuming the zircons crystallized from magmas with Lu/Hf ratios similar to average bulk continental

crust (0.08), are much older, showing peaks around 1.7–1.9 and 2.9–3.1 Ga. Those with the most mantle-like O isotope ratios ($\delta^{18}O < 6.5$) tend to have the older ages, while zircons with higher $\delta^{18}O$ tend to have the younger ages. Presumably, the zircons with the lower $\delta^{18}O$, and older Hf model ages, and represent reworking or melting of deeper crustal material that had never interacted with water at low and moderate temperatures. The important result from this study is that even the zircon ages may date times when older crust was being reworked rather than new crust being formed.

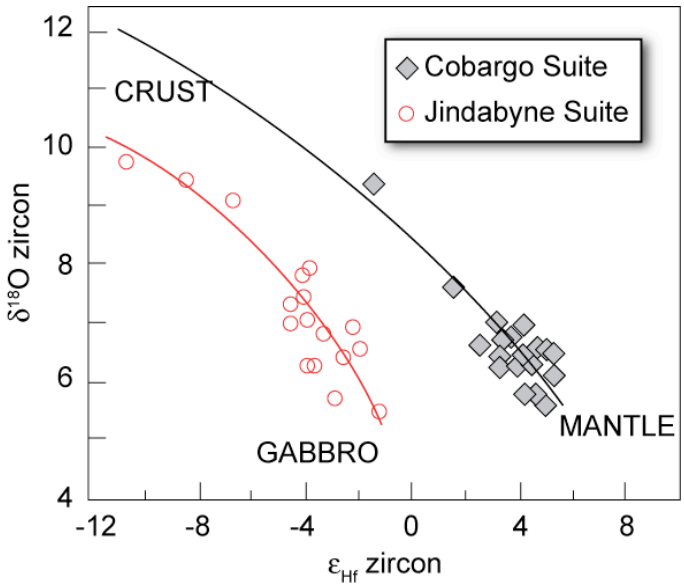

Figure 7.10. $\delta 1^{8}O$ vs. ε_{Hf} for two i-type granite suites from the Lachlan fold belt. They define two distinct mixing curves with a "sedimentary" (high $\delta^{18}O$) material. The average Hf and O isotope (zircon) composition of a gabbro that is spatially associated with the Jindabyne Suite is shown by the star symbol. From Hawkesworth and Kemp (2006).

We should also recognize that rate at which the volume of the continental crust has grown could be different from the rate at which new material has been added to it. This is because crust can also be destroyed. Three mechanisms seem possible. The most easily demonstrated is erosion and subduction of the resulting sediment. A second is subduction erosion, a process is which lower continental crust is essentially abraded away by plate subducting beneath it. A third mechanism is foundering or delamination, particularly of lower crust. The latter process would occur when mafic lower crust becomes dense and mobile enough to sink into the mantle. One possibility would be where the rates of continent creation and destruction are equal, resulting in a steady state volume of continental crust. This is just the situation envisioned by Armstrong (1968, 1971). He argued that although there had been continuing additions to continental crust through geologic time, these additions were balanced by destruction and recycling of continental crust into the mantle so that there had been no net growth of the crust since very early in Earth's history. Armstrong's idea and that of Hurley and Rand frame the range of estimates of the rate of growth of continental crust illustrated in Figure 7.7. To this day, it has not been possible to distinguish unequivocally between these alternatives. The most likely answer, however, lies somewhere between the two extremes.

7.3 Isotopic Composition of the Continental Crust

Isotope systems have particular value in studies of mantle geochemistry because of the difficulty of obtaining direct, representative samples of mantle. The upper crust is largely accessible to direct sampling, so we are less dependent on isotopic composition in geochemical studies of the continental crust. Knowing the isotopic composition of the continental crust is nevertheless useful for (1) establishing the isotopic signature of the continental crust so we can recognize it elsewhere (such as the oceans, atmosphere and mantle) and (2) in mass balance calculations to establish the size of various geochemical reservoirs in the Earth We now turn our attention to assessing the average isotopic composition of the continental crust.

7.3.1 Sediments & Rivers as Samples of the Upper Crust

Chapter 7 The Continental Crust & Oceans

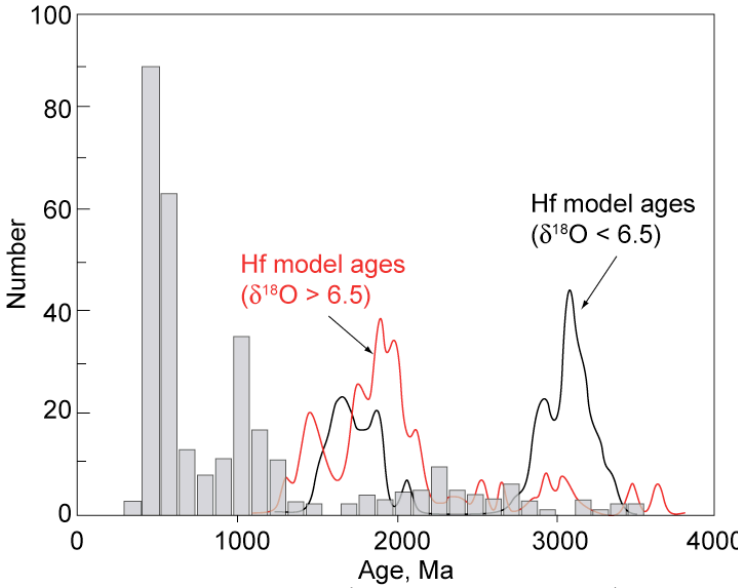

Figure 7.11. Comparison of the crystallization age histogram of detrital zircons from the Lachlan Fold Belt, Australia, as established by ion microprobe U–Pb dating with the distribution of Hf model ages for inherited and detrital zircons with low and approximately mantle-like $\delta^{18}O$ values (>6.5‰) and zircons with high $\delta^{18}O$ values (>6.5‰). Zircons for which Hf and O isotope data are available are from only S-type granites, and two samples of Ordovician metasedimentary rock. After Hawkesworth and Kemp (2006).

The Earth is a big place and obtaining a representative sample of the continental crust is therefore a difficult job. Just as we let nature do some of the work of sampling the mantle for us (by bringing magmas and xenoliths to the surface), we can take advantage of nature's sampling of the crust. Weathering and erosion are constantly removing material from the continents and depositing it in the oceans as sediment. Thus to the isotope geochemist, sediment is a sort of premixed, homogenized, and pre-powdered sample of the continental crust. Figures 7.12 and 7.13 show Sr, Nd and Pb isotopic compositions of marine sediments from the world oceans. The data provide some indication of the composition of the crust. As may be seen, $^{87}Sr/^{86}Sr$ ratios are much higher and $^{143}Nd/^{144}Nd$ isotope ratios much lower than those of the mantle. This is precisely what we expect since we know that Rb and Nd are enriched in the crust relative to Sr and Sm.

U, Th and Pb should also be enriched in the crust in the order Th>U>Pb. Somewhat surprisingly, we find that $^{206}Pb/^{204}Pb$ ratios in the crust overlap the MORB range considerably. $^{207}Pb/^{204}Pb$ ratios are, however, systematically higher. For a given value of $^{206}Pb/^{204}Pb$, $^{208}Pb/^{204}Pb$ ratios in the crust are also systematically higher than in MORB (which are shown in these figures primarily to represent the isotopic composition of the upper mantle), indicating a higher Th/U ratio in the crust as expected. The $^{207}Pb/^{204}Pb$ ratio is an indicator of U/Pb ratios in the early part of Earth's history: the ^{235}U present in the Earth today is only about 2% of the ^{235}U the Earth had at its start: 98% of ^{235}U has already decayed to ^{207}Pb. Half of the ^{235}U had already decayed by 3.8 Ga. So the high $^{207}Pb/^{204}Pb$ of the crust relative to $^{206}Pb/^{204}Pb$ tells us that in the early part of Earth's history, crustal rocks, or their precursors, had a higher U/Pb ratio than the mantle. The half-life of ^{238}U is about the same as the age of the Earth, so $^{206}Pb/^{204}Pb$ has grown more linearly over Earth's history. The similarity of $^{206}Pb/^{204}Pb$ ratios in crust and upper mantle suggests the average U/Pb ratios of the two have been roughly similar over all of Earth's history.

It is appropriate at this point to consider just how representative of the continents the isotopic compositions of marine sediments are. Sediments are only representative of those parts of the crust undergoing erosion. This excludes almost the entirety of the lower crust. So it is therefore proper to consider sediments as representative of only the upper crust. Furthermore, it is likely to be a biased sample of the upper crust. Elevated regions erode faster and therefore generate more sediment than low plains. Tectonically active areas are typically elevated relative to stable areas. By and large, new additions to crust occur exclusively in tectonically active areas and are more likely to be eroded. (By the way, it is exactly this tendency of young igneous crust to be eroded and carried into the oceans that may explain the bias in the zircon data towards zircons created by supercontinent assembly). In essence, this means

sediments will be biased toward younger crust, and will have lower Sr and higher Nd isotope ratios. This biased sampling is to some degree apparent when the data are considered ocean by ocean. The Pacific Ocean is surrounded by tectonically active continental margins, and as we might expect, Sr, Nd, and Pb isotope ratios are lower in Pacific sediments than in those from the Atlantic and Indian. Finally, we need to assure ourselves that when a rock weathers and erodes, the erosion products carried to the sea have isotopic compositions of the rock as a whole. This is probably the case for Nd because it ends up primarily in the clay fraction. A larger fraction of Sr may be carried to the sea as dissolved load; this eventually precipitates in carbonates. However, Sr in seawater is derived in part from the oceanic crust (entering seawater through hydrothermal activity); furthermore carbonates weather easily and much of the riverine and seawater Sr is derived from earlier marine carbonates. Thus the total composition of marine sediments, including both carbonates and detrital fractions is probably not entirely representative of the continental crust.

It is also probable that the Hf carried to the deep ocean is not isotopically representative of the composition of the eroding rock (Patchett et al. 1984; White et al. 1986). This is because much of the Hf in crustal rocks is contained in zircon, which is extremely resistant to weathering. As a result, it is not readily transported great distances from its source. It will typically be retained on the continents in sands and sandstones. That which does reach the sea is mostly deposited on the continental shelf. The Lu/Hf ratio of zircon is lower than that of the bulk rock, so that Hf that does reach the sea may have higher $^{177}Hf/^{176}Hf$ ratios than the eroding rock. Similarly, while much of the ^{204}Pb is probably in phases such as feldspars that break down readily to form clays, the radiogenic isotopes will, to some degree, be

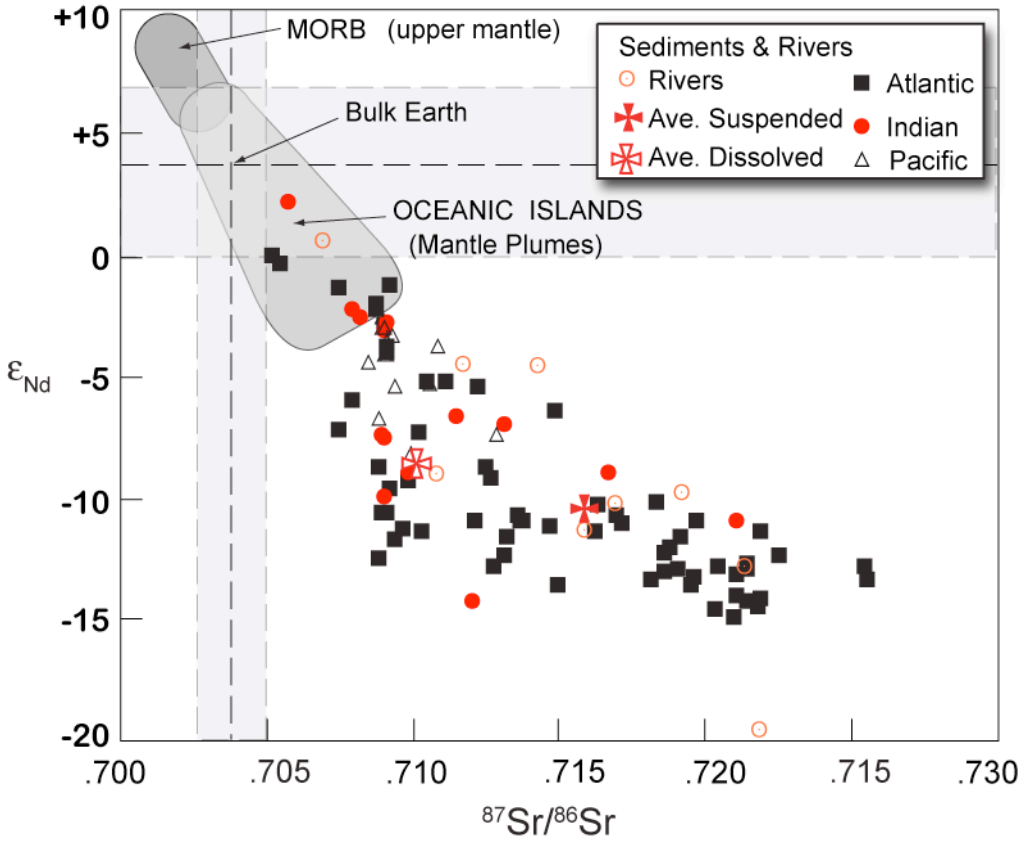

Figure 7.12. Sr and Nd isotope ratios in modern marine sediments (from Ben Othman et al., 1989). Also shown are data on the isotopic composition of suspended loads of rivers (from Goldstein and Jacobsen, 1988), and their estimated global river average ($^{87}Sr/^{86}Sr$ = 0.716; ε_{Nd}=-10.4).

retained in zircon. On the other hand, bedloads of streams, and even the suspended loads, can be biased toward unradiogenic Pb (Garçon et al., 2013), with this material ultimately being retained in the continents. Thus Pb isotope ratios of marine sediment may underestimate $^{206}Pb/^{204}Pb$, $^{207}Pb/^{204}Pb$, and $^{208}Pb/^{204}Pb$ (less so the latter) ratios of the eroding rock. Finally, some of the Pb in marine sediments is also derived from the oceanic crust through hydrothermal activity. In summary, sediments do provide a sample of the continental crust, but it is a biased one. They can nevertheless provide useful information on the composition of the crust today, as well as a perspective on the evolution of the crust through time.

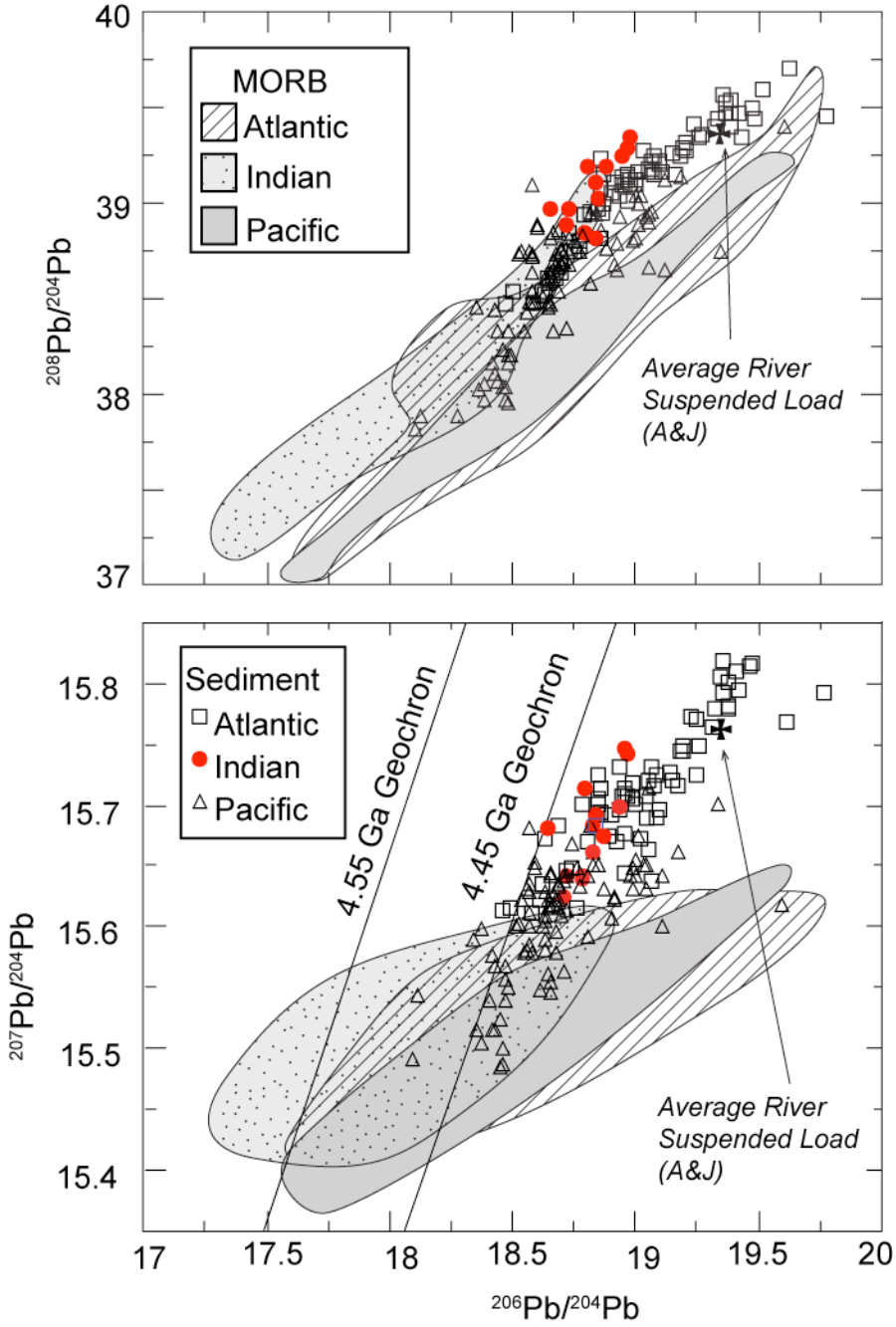

Figure 7.13. Pb isotope ratios in modern marine sediments. Asmeron and Jacobsen's (1993) estimate of the average riverine suspended load is also shown.

A slightly different, but closely related way of estimating crustal composition is to measure the isotopic composition of dissolved or suspended loads in rivers. Rivers carry most of the weathering products from the continents to the oceans (other material is carried by winds and glaciers); hence this strategy is similar to that of sampling oceanic sediments. By using the river samples, we avoid the problem of hydrothermal contributions to sediment. Furthermore, we can calculate weighted averages, based either on the flux of the rivers or the area they drain, to come up with a more accurate estimate of crustal composition than using marine sediments. Goldstein and Jacobsen (1988) measured the riverine Sr and Nd isotopic fluxes by measured isotopic compositions of *suspended load* in a subset of

rivers (mainly North American) and attempting to extrapolate their results to obtain a global average (shown in Figure 7.12). They estimated the $^{87}Sr/^{86}Sr$ and ε_{Nd} of the continental crust exposed to weathering as 0.716 and -10.6 respectively. However, they had no data on a number of major rivers, notably the Brahmaputra, Ganges, and Yangtze. In a related study Goldstein and Jacobsen (1987) also attempted to estimate the global average Sr and Nd isotopic composition of the *dissolved load* of rivers and estimated these as $^{87}Sr/^{86}Sr = 0.7101$ and $\varepsilon_{Nd} = -8.4$ respectively. The much lower Sr isotope ratios in the dissolved load reflects dissolving carbonate sediments. Palmer and Edmond (1989) did a more thorough job of measuring the Sr isotopic compositions of the dissolved load of rivers and obtained an average $^{87}Sr/^{86}Sr$ of 0.7119, but did not measure the Nd isotopic composition. Given the more thorough sampling done by Palmer and Edmond, their estimate is probably more accurate. Since Goldstein and Jacobsen's estimate of average and suspended loads are based on the same rivers sampled at the same locations, it possible, and perhaps likely, that their estimate of the isotopic composition of the suspended load is also a bit low. It is nevertheless the best estimate available.

As we noted above, a small but significant fraction of the Sr in rivers is in dissolved form, whereas the amount of dissolved Nd is insignificant compared to that in the suspended load. Goldstein and Jacobsen (1988) also calculated the bulk load (dissolved plus suspended) carried by rivers. Their estimate of the $^{87}Sr/^{86}Sr$ of the bulk load was 0.7133. The lower $^{87}Sr/^{86}Sr$ in the dissolved fraction reflects the influence of dissolving carbonates, which have lower $^{87}Sr/^{86}Sr$ than silicate rocks because their Rb/Sr is low and seawater, from which they precipitate, is influenced by hydrothermal activity at mid-ocean ridges.

Asmeron and Jacobsen (1993) estimated the Pb isotopic composition of the crust by measuring Pb isotope ratios in the suspended load of sediments, and then estimating the global average from the correlation between Pb isotope ratios and ε_{Nd} in suspended loads. Their estimated composition of the upper crust exposed to weathering is $^{206}Pb/^{204}Pb = 19.32$, $^{207}Pb/^{204}Pb = 15.76$, and $^{208}Pb/^{204}Pb = 39.33$. This mean value is shown in Figure 7.13.

Esser and Turekian (1993) measured the Os isotopic composition of river sediments and from this estimated the average $^{187}Os/^{186}Os$ of the continental crust exposed to weathering at 10.5 ($\gamma_{Os} = 895$). Pegram et al. (1994) measured the isotopic composition of leachable Os in river sediments. The isotopic composition of the leachable fraction presumably reflects isotopic composition of dissolved Os (which was in too low a concentration to measure directly). $^{187}Os/^{186}Os$ ranged from 10.1 to 21.5.

Using riverine suspended load eliminates the influence of hydrothermal activity on marine sediments, but the other problems with using sediments to estimate continental material remain: at best we can only estimate the composition

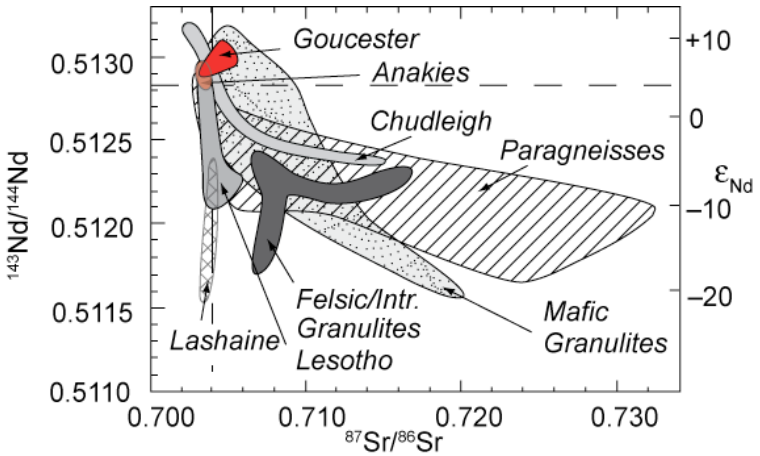

Figure 7.14. Sr and Nd isotopic composition of granulite† xenoliths in volcanic rocks. Chudleigh, Gloucester, and Anakies are in Australia, Lashaine is in Tanzania, and Lesotho is in South Africa. From Rudnick (1992).

† granulite is a high-grade, largely anhydrous, metamorphic rock. It most commonly contains plagioclase and pyroxene as essential minerals, and may sometimes contain garnet. A paragneiss is a rock derived from a sedimentary precursor.

of the crust exposed to weathering.

7.3.2 Isotopic Composition of the Lower Crust

Like the mantle, the lower continental crust is not generally available for sampling. While much can be learned about the lower crust through remote geophysical means (seismic waves, gravity, heat flow, etc.), defining its composition and history depends on being able to obtain samples of it. As with the mantle, three kinds of samples are available: terranes or massifs that have been tectonically emplaced in the upper crust, xenoliths in igneous rocks, and magmas produced by partial melting of the lower crust. All these kinds of samples have been used and each has advantages and disadvantages similar to mantle samples. We will concentrate here on xenoliths and terrains.

Figure 7.14 summarizes Sr and Nd isotopic compositions of lower crustal xenoliths. Initial Sr and Nd isotopic studies of the lower crust indicated it had similar ε_{Nd} to the upper crust, but low $^{87}Sr/^{86}Sr$. It is clear from Figure 7.14 that while this may be true in some instances, the lower crust is quite heterogeneous in its isotopic composition and is not easily characterized by a single isotopic composition. Some lower crustal xenoliths have very radiogenic Sr.

The Pb isotopic composition of the lower crust is a particularly important question because it bears on the question of the composition of the bulk silicate Earth and its age. The upper crust, the upper mantle, and mantle plumes all have Pb isotopic compositions lying to the right of the 4.5 Ga Geochron. If the Earth is this old, mass balance requires a significant reservoir of unradiogenic Pb, i.e., Pb that plots to the left of the Geochron somewhere in the Earth. Some early studies of granulite terrains, such as the Scourian in Scotland, suggested the lower crust might be characterized by unradiogenic Pb. Furthermore, the lower crust is known to have a low heat production, implying low concentrations of U and Th.

Rudnick and Goldstein (1990) found that while most Archean lower crustal terrains did indeed have very unradiogenic Pb, post-Archean ones did not. This is summarized in Figure 7.15. Furthermore, many lower crustal xenoliths have radiogenic Pb (Figure 7.16). Rudnick and Goldstein concluded that unradiogenic Pb can only develop in regions that have remained stable for long time periods, i.e., only in cratons. In areas where orogenies have occurred subsequent to crust formation, the Pb isotopic composition of the lower crust is rejuvenated trough mixing with radiogenic Pb from upper crust and mantle-derived magmas.

Rudnick and Goldstein (1990) attempted to estimated the average Pb isotopic composition of the lower crust based on this orogenic age—Pb isotopic composition relationship. Their estimate is compared with other estimates for the Pb iso-

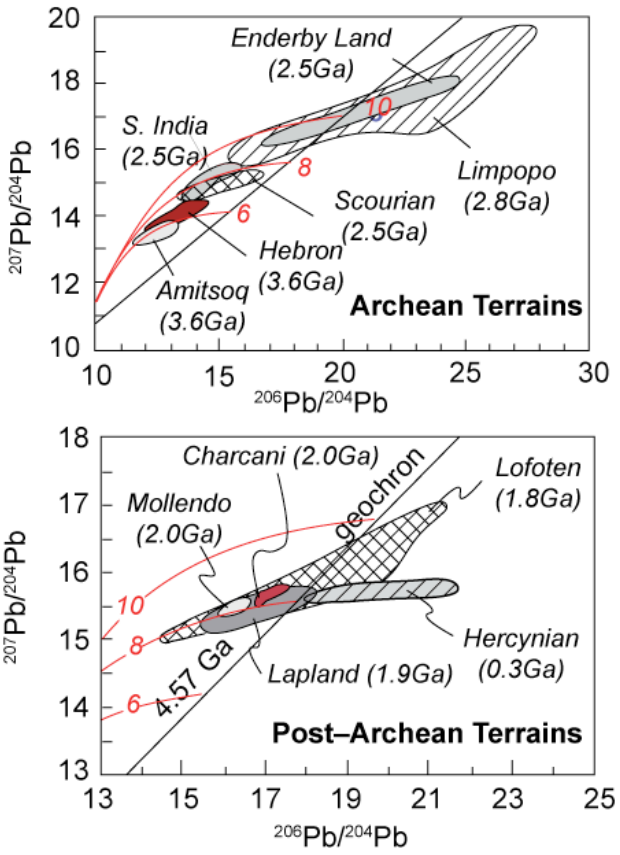

Figure 7.15. Pb isotope ratios in Archean and post-Archean granulite (i.e., lower crustal) terrains. the 4.57 Ga geochron and single stage growth curves for $\mu = 6$, $\mu = 8$, and $\mu = 10$ are also shown. While Archean terrains appear to be characterized by unradiogenic Pb, this is less true of post-Archean terrains. After Rudnick and Goldstein (1990).

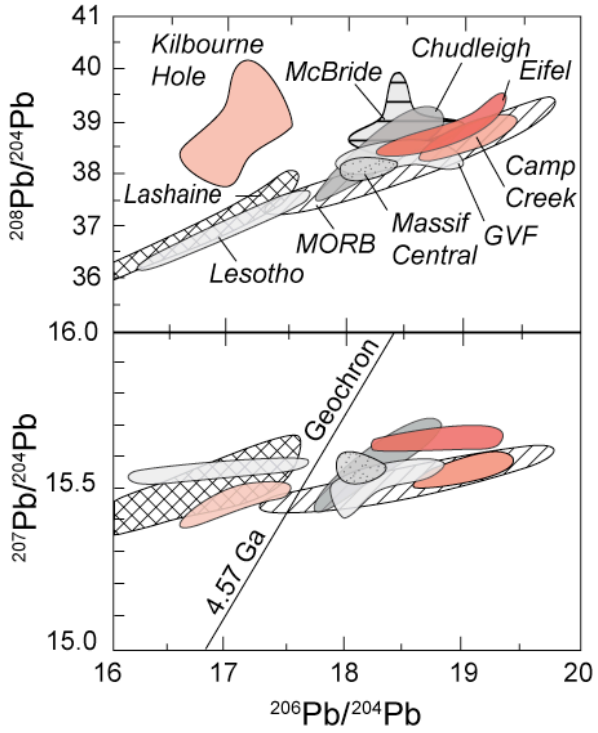

Figure 7.16. Pb isotope ratios in lower crustal xenoliths. Eifel is in Germany; GVF (Geronimo Volcanic Field), Kilbourne Hole and Camp Creek in the southwest US, McBride in Australia; and the Massif Central, in France. From Rudnick and Goldstein (1990).

For example, the well-known work of Taylor and McLennan (1985, 1995) is based largely on sampling of the Canadian Precambrian Shield and the assumption that the crust is ultimately andesitic in composition. Taylor and McLennan (1995) estimated the $^{232}Th/^{238}U$ ratio (κ) of the crust to be 3.87, a value that is surprisingly low given the value for the bulk Earth is 4.0±0.2 and Th isotope ratios indicate that κ in the depleted mantle is ~2.5. Rudnick and Fountain (1995) estimated a value of 3.97, also surprisingly low, but perhaps not surprising since it was based in part of the work of Taylor and McLennan. If the mantle has lower κ than the bulk Earth, then mass balance would seem to require that the crust should have a high value than the bulk Earth. Furthermore, crustal rocks tend to have higher $^{208}Pb^*/^{206}Pb^*$, suggesting κ has been higher in the crust than in the topic composition of the upper and lower crust in Figure 7.17 Rudnick and Goldstein concluded that while the Pb of the lower crust does lie to the left of the 4.57 Ga Geochron, it is not sufficiently unradiogenic to balance the unradiogenic Pb of the upper crust and upper mantle. Figure 7.17 also shows Halliday's (2004) average of a number of estimates of the Pb isotopic composition of the bulk silicate Earth. The average lies clearly to the right of the 4.57 Ga Geochron, but close to a 4.45 Ga Geochron. Thus the apparent Pb isotopic composition of the Earth is consistent with evidence we discussed earlier that accretion of the Earth was not complete until roughly 100 Ma after the beginning of the solar system.

7.3.3 Pb Isotope Ratios and the Th/U Ratio of the Crust

There have been a number of attempts to estimate the bulk composition of the continental crust. Isotope ratios can be used to check and refine estimates of these. Estimates of crustal composition are generally based on compilations of compositional data over wide, but nevertheless limited, areas of the continental crust. Model-based assumptions are often required to transform these limited data sets into estimates of the composition of the entire crust.

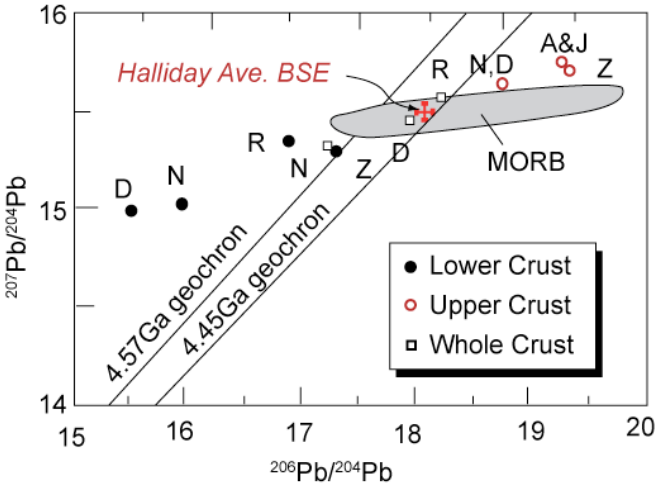

Figure 7.17. Estimates of the Pb isotopic composition of the crust: N: Newsom et al. (1986), D: Davies (1984), Z: Zartman and Doe (1981), R: Rudnick and Goldstein (1990). Also shown is Halliday's (2004) average of bulk silicate Earth estimates.

mantle for geologically long times.

Paul et al. (2003) used Asmeron and Jacobsen's (1993) estimate of the Pb composition of the riverine flux to estimate the Pb isotopic composition of upper crust and data from Rudnick and Goldstein (1990) to estimate the Pb isotope composition the lower crust. From this they calculated a κ_{Pb} for the crust of 4.26-4.30. This clearly implies the κ value of the crust must be higher than that estimated by Taylor and McLennan and Rudnick and Fountain. Indeed, when one considers that the crust is derived from the mantle, and the mantle source of crustal rocks have a κ equal to or lower than the bulk Earth value of ~4, this implies a κ substantially higher than ~4. Paul et al. used a mathematical model of the isotopic evolution of the Earth to estimate just how much higher. As is illustrated in Figure 7.16, the estimated that κ in the crust is 5.17. That value actually agrees well with an estimate of Wedepohl (1995). Notice that the model also correctly predicts a large difference between the κ_{Th} and κ_{Pb} in the depleted mantle, consistent with the observation of Galer and O'Nions (1985). The increase in κ_{Pb} in the depleted mantle in the model results from recycling crust Pb into the mantle through subduction.

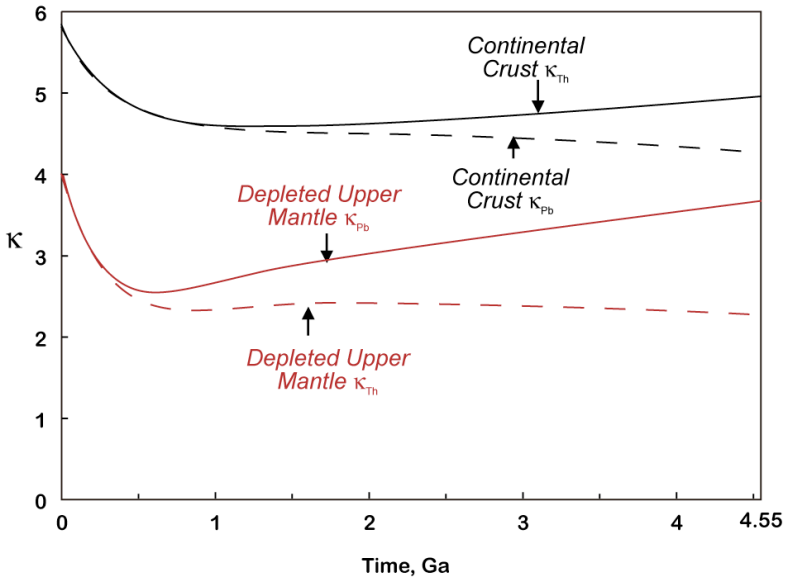

Figure 7.18. Computed evolution of κ and κ_{Pb} in the crust and depleted mantle. A present day κ_{Pb} in the crust of 4.3 requires a κ of 5.17, because some of the Pb now in the crust would have resided in the mantle, which has low κ. After Paul et al. (2003).

7.4 Other Approaches to Crustal Composition and Evolution

As we have seen, samples of particulate material in rivers can be used to obtain estimates of upper crustal composition. However, because the Sm/Nd ratio changes little during production of sediment, these sediment samples also contain information on the age of the rocks they are derived from through Nd model ages (or crustal residence time). Sm/Nd and $^{143}Nd/^{144}Nd$ ratios in major rivers draining about 25% of the exposed continental crust (excluding Antarctica and Australia) as well as

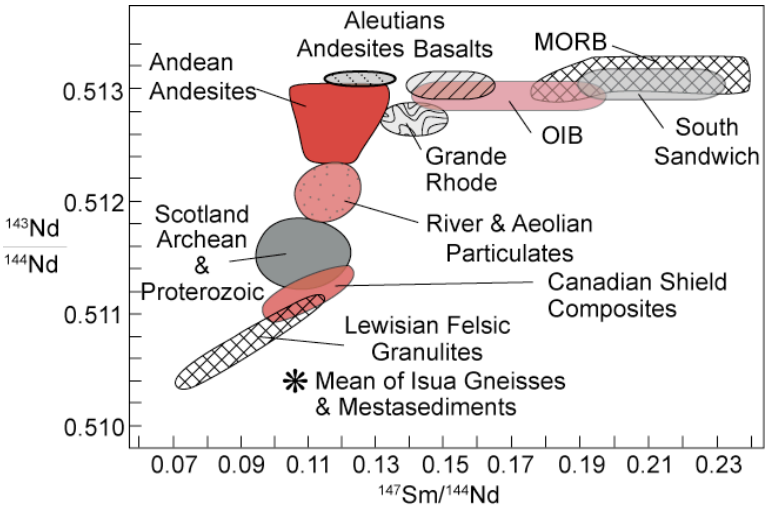

Figure 7.20. $^{147}Sm/^{144}Nd$ and $^{143}Nd/^{144}Nd$ in various crustal and mantle-derived rocks (from Goldstein and O'Nions, 1984).

samples of loess and aeolian dusts were analyzed by Goldstein and O'Nions (a different Steve Goldstein than the Steve Goldstein of the Goldstein and Jacobsen papers) are shown in Figure 7.19. The Nd isotope ratios are fairly homogeneous. Sm/Nd ratios are quite uniform, illustrating a point that was already well known, namely that rare earth patterns of continental crustal material show relatively little variation. A further illustration of this point is shown in Figure 7.20. Virtually all crustal rocks have $^{147}Sm/^{144}Nd$ ratios at the extreme end of the range observed in mantle-derived rocks, and the range of $^{147}Sm/^{144}Nd$ ratios in crustal material is small compared to the range observed in mantle-derived rocks. Figure 7.20 suggests there is a major fractionation of the Sm/Nd when crust is formed from the mantle, but thereafter processes within the crust tend to have only second-order effects on the Sm/Nd ratio. This is the main reason why crustal residence time calculated from $^{147}Sm/^{144}Nd$ and $^{143}Nd/^{144}Nd$ is such a robust parameter.

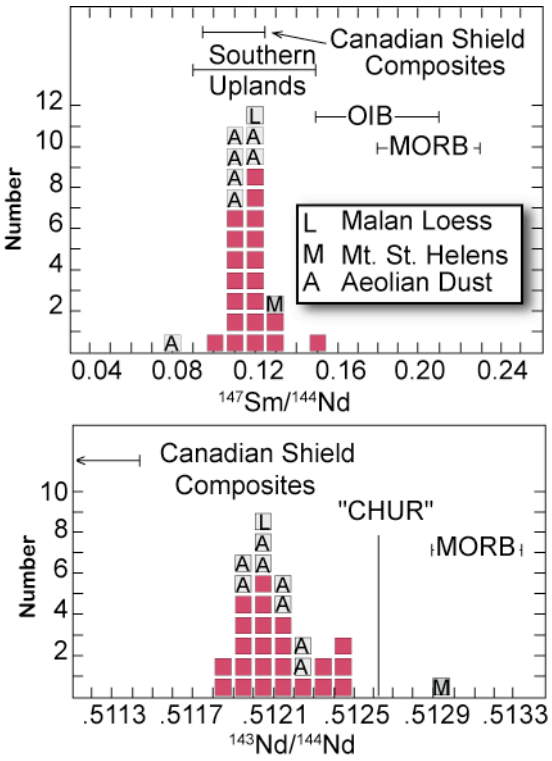

Figure 7.19. $^{147}Sm/^{144}Nd$ and $^{143}Nd/^{144}Nd$ ratios in major rivers, aeolian dusts, and loess (from Goldstein and O'Nions, 1984).

By studying sediments of various ages, we should be able to draw some inferences about the rates of continental growth. Goldstein and O'Nions (1984) found that the mean crustal residence time (τ_{DM}, calculated from $^{147}Sm/^{144}Nd$ and $^{143}Nd/^{144}Nd$) of the river particulates they studied was 1.7 Ga, which they interpreted as the mean age of the crust being eroded. However, they estimated the mean crustal residence time of the entire sedimentary mass to be about 1.9 Ga. Figure 7.21 compares the stratigraphic age* of sediments with their crustal residence ages. Note that in general we expect the crustal residence age will be somewhat older than the stratigraphic age. Only when a rock is eroded into the sedimentary mass immediately after its derivation from the mantle will its stratigraphic (τ_{ST}) and crustal residence age (τ_{CR}) be equal.

The top diagram illustrates the relationships between τ_{ST} and τ_{CR} that we would expect to see for various crustal growth scenarios, assuming there is a relationship between the amount of new material added to the continents and the amount of new material added to the sedimentary mass. If the continents had been created 4.0 Ga ago and if there had been no new additions to continental crust since that time, then the crustal residence time of all sediments should be 4.0 Ga regardless of stratigraphic age, which is illustrated by the line labeled 'No New Input'. If, on the other hand, the rate of continent growth through time has been uniform since 4.0 Ga, then τ_{ST} and τ_{CR} of the sedimentary mass should lie along a line with slope of 1/2, which is the line labeled 'Uniform Rate'. The reason for this is as follows. If the sedimentary mass at any given time samples the crust in a representative fashion, then τ_{CR} of the sedimentary mass at the time of its deposition (at τ_{ST}) should be $(4.0-\tau_{ST})/2^{\dagger}$, i.e., the mean time between

* The stratigraphic age is the age of deposition of the sediment determined by conventional geochronological or geological means.

† One way to rationalize this equation is to think of newly deposited sediment at τ_{ST} as a 50-50 mixture of material derived from the mantle at 4.0 Ga and τ_{ST}. The equation for the T_{CR} of this mixture would be:

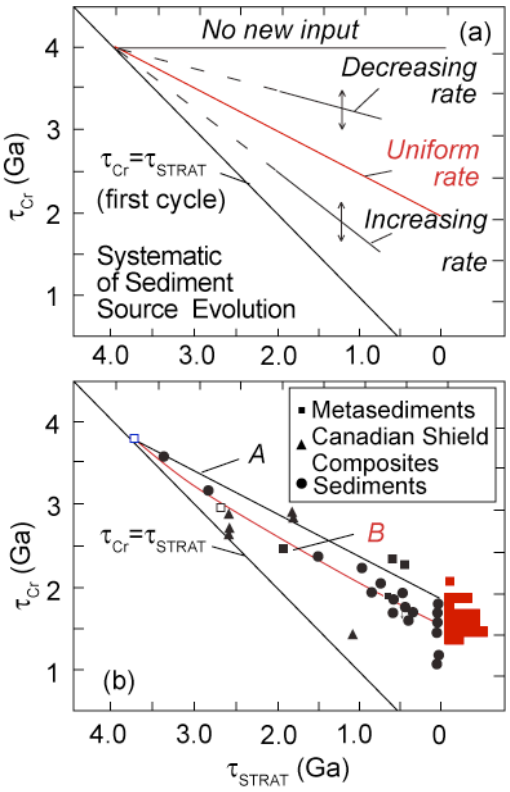

Figure 7.21. Relationship between stratigraphic age of sediments and the crustal residence age of material in sediments. See text for discussion (from Goldstein and O'Nions, 1984).

the start of crustal growth (which we arbitrarily assume to be 4.0 Ga) and τ_{ST}. A scenario where the rate of crustal growth decreases with time is essentially intermediate between the one-time crust creation at 4.0 and the uniform growth rate case. Therefore, we would expect the decreasing rate scenario to follow a trend intermediate between these two, for example, the line labeled 'Decreasing Rate'. On the other hand, if the rate has increased with time, the τ_{CR} of the sedimentary mass would be younger than in the case of uniform growth rate, but still must be older than τ_{ST}, so this scenario should follow a path between the uniform growth rate case and the line $\tau_{ST} = \tau_{CR}$, for example, the line labeled 'Increasing Rate'.

Line A in Figure 7.21b is the uniform growth rate line with a slope of 1/2. Thus the data seem to be compatible with a uniform rate of growth of the continental crust. However, the situation is complicated by various forms of recycling, including sediment-to-sediment and sediment-to-crystalline rock, and crust-to-mantle. Goldstein and O'Nions noted sedimentary mass is cannibalistic: sediments are eroded and redeposited. In general, the sedimentary mass follows an exponential decay function with a half-mass age of about 500 Ma. This means, for example, that half the sedimentary mass was deposited within the last 500 Ma, the other half of the sedimentary mass has a depositional age of over 500 Ma. Only 25% of sediments would have a depositional ('stratigraphic') age older than 1000 Ma, and only 12.5% would have a stratigraphic age older than 1500 Ma, etc. Line B represents the evolution of the source of sediments for the conditions that the half-mass stratigraphic age is always 500 Ma and this age distribution is the result of erosion and re-deposition of old sediments. The line curves upward because in younger sediments consist partly of redeposited older sediments. In this process, τ_{ST} of this cannibalized sediment changes, but τ_{CR} does not. Goldstein and O'Nions noted their data could also be compatible with models, such as that of Armstrong, which have a near constancy of continental mass since the Archean if there was a fast but constantly decreasing rate of continent-to-mantle recycling.

We should emphasize that the τ_{CR} of sediments is likely to be younger than the mean age of the crust. This is so because sediments preferentially sample material from topographically high areas and topographically high areas tend to be younger than older areas of the crust (e.g. the shields or cratons) be-

---

$$\tau_{CR} = \frac{4.0 + \tau_{ST}}{2}.$$

At time of deposition, its crustal residence age would have been: $\tau_{CR} = \frac{4.0 + \tau_{ST}}{2} - \tau_{ST} = \frac{4.0\tau_{ST}}{2}$.

You could satisfy yourself that a mixture of material having τ_{CR} of all ages between 4.0 Ga and τ_{ST} would have the same τ_{CR} as given by this equation.

cause young areas tend to be still relatively hot and therefore high (due to thermal expansion of the lithosphere).

7.5 Subduction Zones

7.5.1 Geochemistry of Two-Component Mixtures

Subduction-related magmatism is probably the principle way in which new material is added to the continental crust at present. Such magmas are, however, often mixtures of mantle-derived and crust-derived components. Thus before exploring their isotope geochemistry, we need to consider the effects of mixing on isotope ratios.

When two components contribute material to magmas, we might expect that the proportion contributed by each might vary. If we plot the concentration of any two elements in different samples of this mixture against each other, they must lie on a straight line between the two end members. However, if we plot ratios of either elements or isotopes, they need not lie on a straight line. Indeed, in the general case they do not; rather they will define a curve whose equation is:

$$A\left(\frac{p}{P}\right)+B\left(\frac{p}{P}\right)\left(\frac{q}{Q}\right)+C\left(\frac{q}{Q}\right)+D=0 \qquad 7.1$$

Where ratios q/Q and p/P are the variables of the abscissa and ordinate respectively. If end members are designated 1 and 2 and have ratios $(q/Q)_1$ and $(p/P)_1$, and $(q/Q)_2$ and $(p/P)_2$ respectively, then

$$A=Q_2P_1\left(\frac{q}{Q}\right)_2-Q_1P_2\left(\frac{q}{Q}\right)_1 \qquad 7.2$$

$$B=Q_1P_2-Q_2P_1 \qquad 7.3$$

$$C=Q_2P_1\left(\frac{p}{P}\right)_2-Q_1P_2\left(\frac{p}{P}\right)_1 \qquad 7.4$$

$$D=Q_1P_2\left(\frac{p}{P}\right)_2\left(\frac{q}{Q}\right)_2-Q_2P_1\left(\frac{p}{P}\right)_1\left(\frac{q}{Q}\right)_1 \qquad 7.5$$

The curvature of the mixing line will depend on the ratio r:

$$r = (Q_1P_2)/(Q_2P_1) \qquad 7.6$$

The greater the value of r, the greater the curvature. Only in the special case were r=1 is the line straight. This is illustrated in Figure 7.22. This result is completely general and applies to mixing of river water and seawater, etc. as well as mixing of magmas.

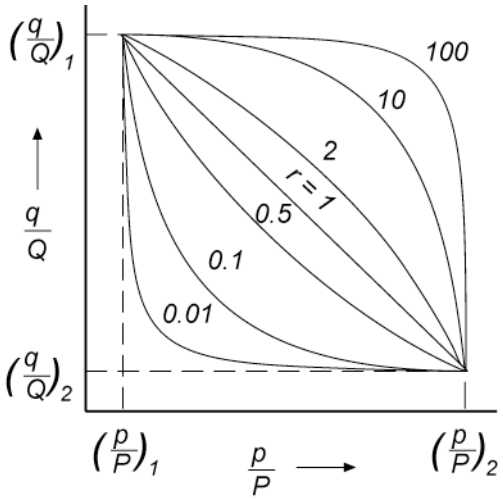

Figure 7.22. Plots of ratios of elements or isotopes, q/Q versus p/P for mixing of end members 1 and 2. The numbers along the curves are the values for r.

Taking a concrete example, if our plot is $^{143}Nd/^{144}Nd$ versus $^{87}Sr/^{86}Sr$, then the curvature depends on the ratio of $(^{144}Nd_1{}^{86}Sr_2)/(^{144}Nd_2{}^{86}Sr_1)$. Since in most instances the amount of ^{144}Nd and ^{86}Sr is to a very good approximation proportional to total Nd and Sr, respectively, r is approximated by Nd_1Sr_2/Nd_2Sr_1. If we express this ratio as $r = (Nd/Sr)_1/(Nd/Sr)_2$ we see that the curvature depends on the ratio of the Nd/Sr ratio in the two end members. In mantle-derived rocks Sr/Nd ~ 10, so mixing curves typically show only modest curvature. In crustal rocks and sediments, deviations from r = 1 are more likely and curved mixing lines therefore more common.

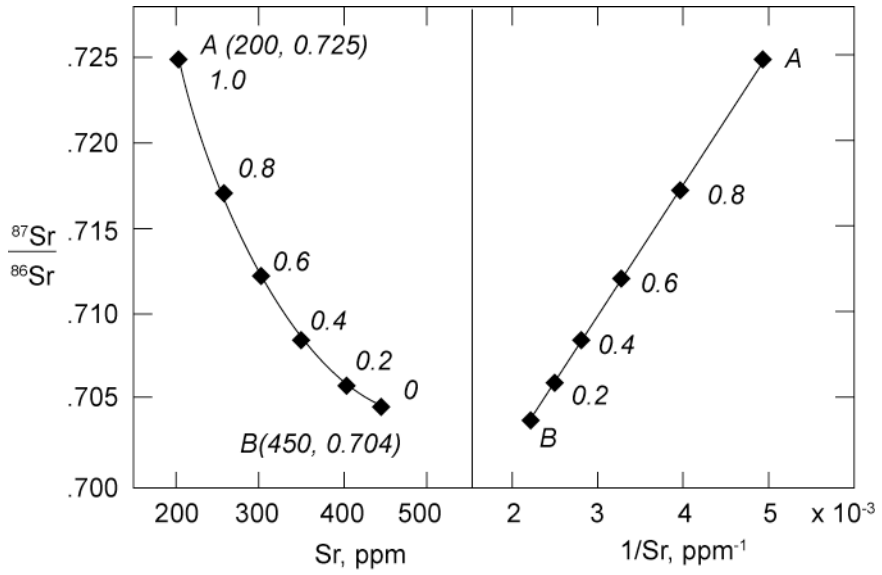

Figure 7.23. Mixing hyperbola formed by components A and B. After Faure (1986).

Note that r will always be 1 where $Q = P$, that is, where the two denominators are the same. Consequently, on $^{207}Pb/^{204}Pb$—$^{206}Pb/^{204}Pb$ plots mixing curves will always be straight lines because the denominators are the same (i.e., $Q = P = {}^{204}Pb$).

Two component mixtures will also form straight lines when we plot a radiogenic isotope ratio vs. a parent-daughter ratio, i.e., on isochron plots, e.g., $^{87}Sr/^{86}Sr$—$^{87}Rb/^{86}Sr$, because the denominators are the same. Thus mixing lines can be mistaken for isochrons and visa versa. One way to distinguish the two is a ratio-element plot. A ratio-element plot, for example $^{87}Sr/^{86}Sr$ vs. Sr, will also in general be a curved line described by equation 7.1 (because the denominators are ^{86}Sr and 1), but a ratio plotted against the inverse of the denominator, for example $^{87}Sr/^{86}Sr$—1/Sr, will be a straight line (at least to the degree that ^{86}Sr is proportional to total Sr, which will be the case where the range in $^{87}Sr/^{86}Sr$ ratios is small). Such a plot can be a useful discriminator between isochrons and mixing lines because only in the latter case will $^{87}Sr/^{86}Sr$—1/Sr necessarily define a straight line (Figure 7.23). Again, this result is completely general, and while the general principals have been illustrated with isotope ratios, they apply equally well to elemental ratios.

When the compositions of a magma or series of magmas appear to reflect mixing, we are often faced with having to decide whether (1) two mantle-derived magmas are mixing, (2) two distinct mantle sources are mixing, or (3) a mantle-derived magma is mixing with assimilated crust. In case (2), plots involving an elemental concentration will not fall on mixing lines because partial melting and fractional crys-

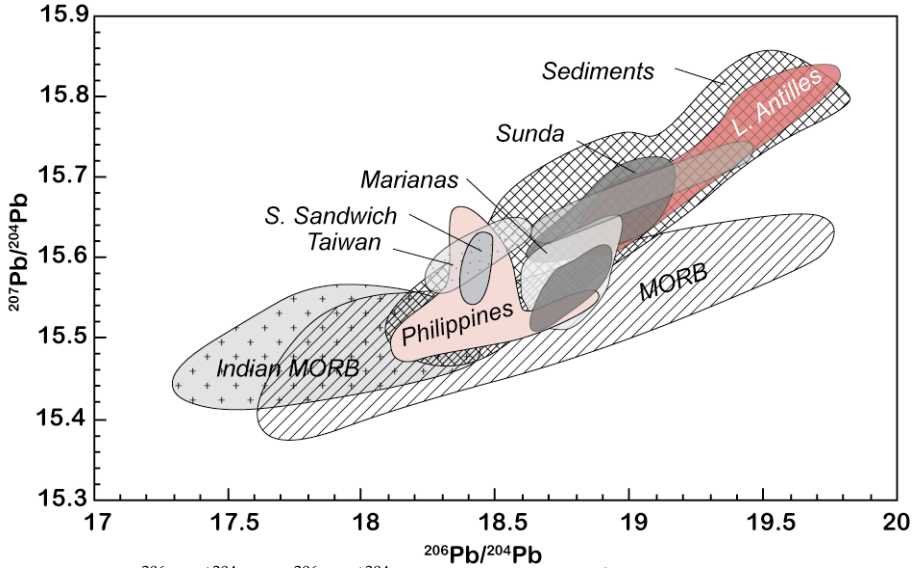

Figure 7.24. $^{206}Pb/^{204}Pb$—$^{206}Pb/^{204}Pb$ for 3 arcs and the sediments available for subduction beneath them. In each case, the arcs define an array between MORB and the associated sediment.

tallization will change element concentrations. Isotope ratios will not be changed by magma genesis so a plot of two isotope ratios will describe a mixing line in case (2) as well as case (1).

Case (3), assimilation of crust by mantle-derived magmas presents a more difficult problem. Recognizing crustal assimilation in subduction zones magmas can be particularly difficult because many of geochemical effects characteristic of crustal assimilation can also result from the presence of subducted sediment component in such magmas. Plots of two isotope ratios will define a straight line in assimilation provided the process is simple mixing and does not involve simultaneous melting or crystallization. However, assimilation generally *does* involve melting and crystallization and produces more complicated ratio-ratio variations. Stable isotope ratios, oxygen in particular, are useful in recognizing assimilation. This is so because the mantle tends to have uniform stable isotope ratios and ones that differ from those in crustal rocks. We will postpone a full discussion of assimilation until Chapter 9.

7.5.2 Isotopic Compositions of Subduction-Related Magmas

As we noted, subduction zone magmatism is probably the principal mechanism by which new crust has been created in the Phanerozoic, and perhaps throughout geologic time. In addition, subduction zones are the regions in which oceanic crust and its veneer of sediment are recycled into the mantle. Given the obvious importance of subduction zones in the evolution of the Earth, it is worth briefly considering the isotope geochemistry of subduction-related magmas.

Island-arc and continental margins volcanics (IAV) are distinctive in many of their geochemical features. Isotopic studies have now demonstrated one reason for this: their sources contain a component of subducted oceanic crust and sediment. The first evidence to this effect was a study of Pb isotope ratios in the Lesser Antilles by Armstrong in 1971. Figure 7.24 compares Pb isotope ratios in a number of arcs to those of MORB and sediments. The similarity between the arc magmas and the sediments, first noted by Armstrong, is striking and certainly not coincidental. The sediment, or rather some part of it, is being subducted to depths of 100 km beneath the arc where it enters the magma source region. In

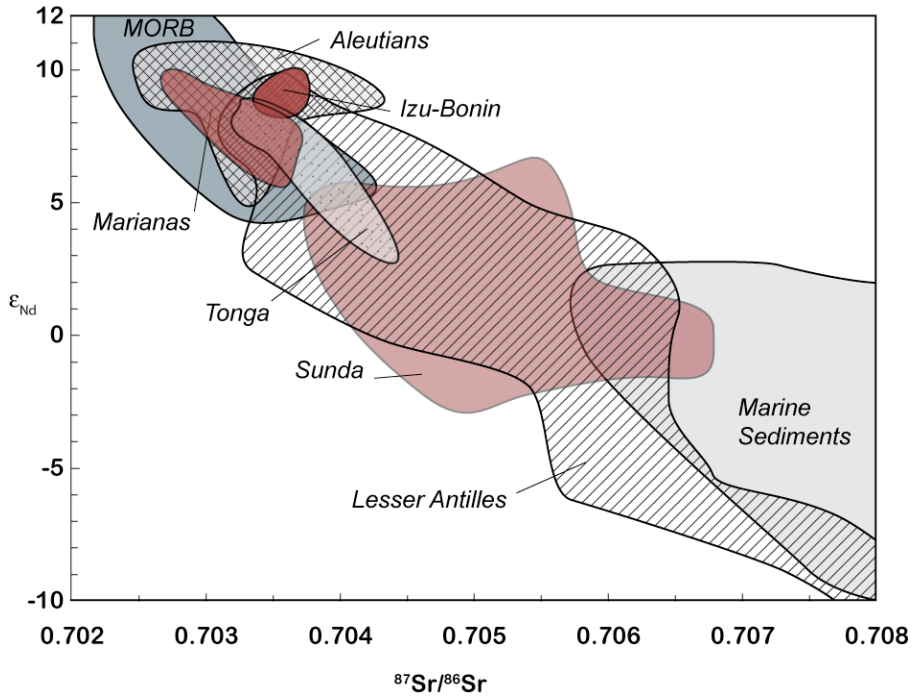

Figure 7.25. ε_{Nd} vs $^{87}Sr/^{86}Sr$ in intra-oceanic island arcs. Based on data in the GEOROC database.

terms of their Sr-Nd systematics, however, island arcs overlap the MORB and OIB fields considerably (Figure 7.25), although they have some tendency to plot to the high $^{87}Sr/^{86}Sr$ side. This may be because the subducted oceanic crust is also an important source of Sr and Nd. The Nd of old (< 150 Ma) oceanic crust will not be very different isotopically from that of modern MORB. However, hydrothermal activity at mid-ocean ridges results in isotopic exchange between basalt and seawater, shifting the $^{87}Sr/^{86}Sr$ of the oceanic crust to higher values (mean value of altered oceanic crust is probably in the range of 0.703-0.7035). One can also see from Figure 7.26, that Sr and Nd in island arc volcanics can qualitatively be described as a mixture of altered oceanic crust, depleted mantle, and sediment. In some cases, however, anomalous mantle, similar to that of mantle plumes, may also be involved.

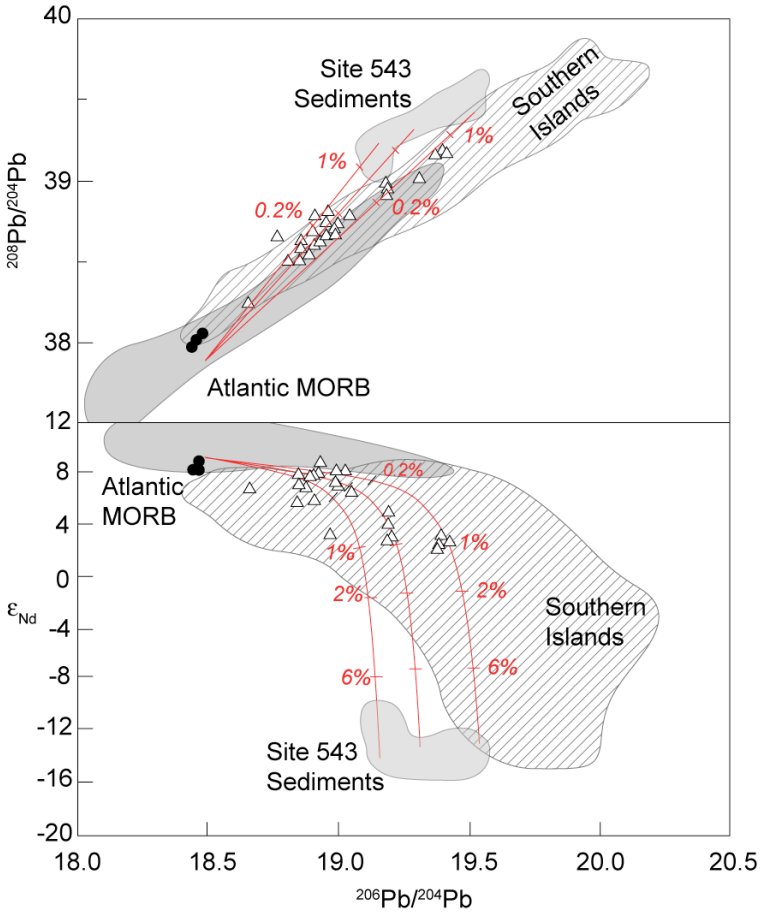

Figure 7.26. Pb and Nd isotopic compositions of lavas from the northern and southern parts of the Lesser Antilles arc compared with those of Site 543 sediments and Atlantic MORB. Data from the northern islands are shown as open triangles, basalts from Hole 543 are shown as solid circles. The solid lines represent mixing curves between depleted mantle (ave. MORB) and Site 543 sediments. Ticks show the percentage of sediments in the mixture. Compositions of the end-members used for the calculation: (1) depleted mantle: Nd = 0.71 ppm, Pb=0.023 ppm, $^{143}Nd/^{144}Nd$=0.5131, $^{206}Pb/^{204}Pb$ =18.5, and $^{208}Pb/^{204}Pb$=37.9; (2) for the sediment end members, Nd and Pb concentrations are those of the average of the entire Site 543 sedimentary pile and the isotopic compositions of the three end members are two samples from Site 543 and the average of Site 543. From Carpentier et al. (2008).

Thus arc magmas are themselves mixtures of mantle and crustal material, and continental margin volcanism, or accretion of intra-oceanic arcs, involves both additions of new material from the mantle and recycling of older crust. The proportion of sediment in arc magma sources can be estimated from mixing models (e.g., Figure 7.26) and is generally quite small, typically a percent or two or less. Nevertheless, because sediment has much higher concentrations of Sr, Nd, and particularly Pb than mantle, significant proportions of these elements, and sometimes most of the Pb, are derived from the sediment. Continental margin magmas, such as those of the Andes, generally assimilate some of the crust through which they ascend, which results in further reworking, or high-level recycling, of continental crust.

Interestingly, the Lesser Antilles may be something of a present-day analogy to the isotopic pattern in the southwest US that we discussed above (Figure 7.8). The arc is built perpendicular to the continental

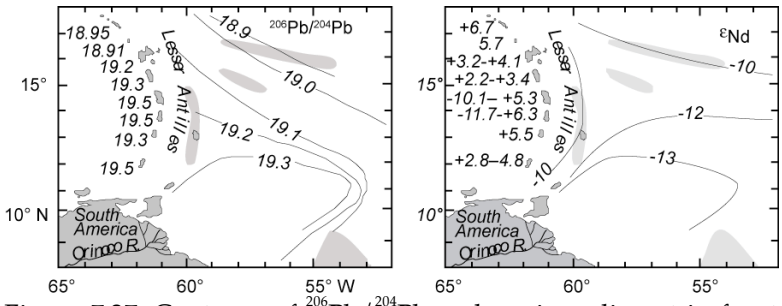

Figure 7.27. Contours of $^{206}Pb/^{204}Pb$ and ε_{Nd} in sediment in front of the Lesser Antilles island arc. Range or mean of these parameters in Lesser Antilles arc volcanics is written adjacent to each island (after White and Dupré, 1986).

margin (an unusual situation). Archean crust occurs in the Guiana highland, which is drained by the Orinoco River, which has deposited a considerable volume of sediment in front of the arc. Because of the age of the drainage basin, the sediment of the Orinoco contains particularly radiogenic Pb and Sr and unradiogenic Nd. Isotopic compositions in the sediment grade northward (Figure 7.27). This northward variation is mirrored by in the isotopic composition of arc lavas, and reflects a decreasing continental contribution with distance from the continent.

7.5.2.1 ^{10}Be in Arc Lavas

If further evidence of the presence of subducted sediment in arc magmas is needed, it is provided by yet another isotopic system: ^{10}Be. We have discussed how ^{10}Be is created by spallation in the atmosphere. Because of its half-life is only 1.6 Ma, and cosmic rays penetrate solid matter so poorly, cosmogenic Be should not to be present in the interior of the Earth. Yet it is present in IAV (Figure 7.28). A skeptic might suppose that some unknown neutron reaction can create ^{10}Be in the Earth's interior. In addition, cosmogenic ^{10}Be in rain is rapidly absorbed onto clays, and that skeptic might suppose that even very young lavas might also absorb ^{10}Be. For these reasons, it was important to do control experiments by measuring ^{10}Be in non-arc lavas. As Figure 17.28 shows, ^{10}Be is not present in non-arc lavas. Thus the only reasonable interpretation of ^{10}Be in arc magmas is that it is derived from subducted sediment.

Not all arc lavas have ^{10}Be. For example, there is no ^{10}Be in lavas from the Lesser Antilles, where Pb and other isotopes suggest a significant contribution from sediment. The same is true of the Sunda arc. In both these arcs, however, the sediment pile is so thick that most sediment is accreted in a forearc wedge rather than subducted. In the Lesser Antilles, seismic and other studies of the forearc show that only the lowermost 100 m or so of sediment is carried into the subduction zone and possibly subducted. These are pre-Miocene sediments. Using our rule of thumb that a radioactive isotope will be gone after 5 to 10 half-lives, we can predict that sediment older

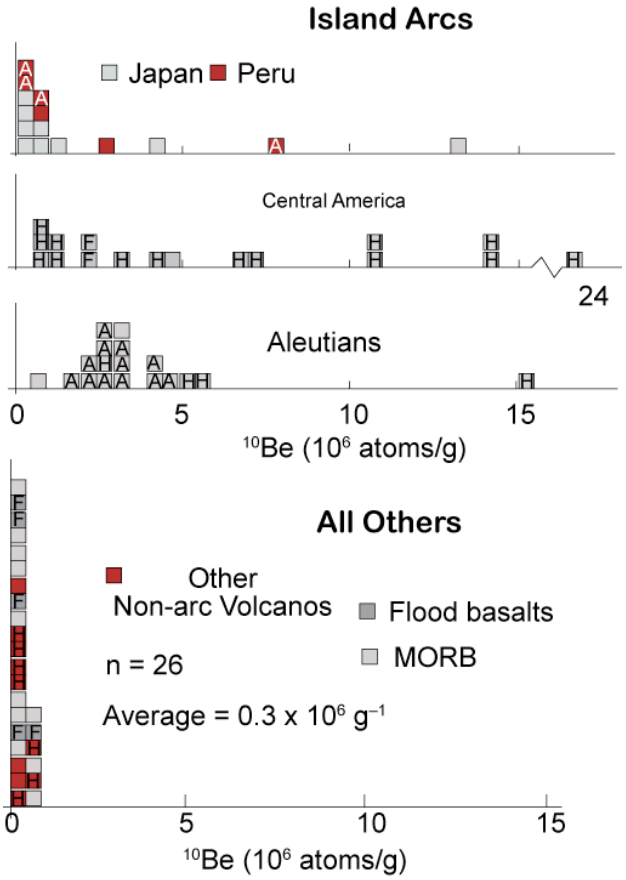

Figure 7.28. Comparison of ^{10}Be contents in arc (left) and non-arc (right) lavas (from Tera et al., 1986). "A" indicates sample from active volcano, "H" a historic eruption, and "F" (fresh) indicates collected during eruption.

than 8 to 16 Ma should have no ^{10}Be. Thus it is no surprise that ^{10}Be is not present in Lesser Antilles magmas.

7.5.2.2 Th Isotope Geochemistry of Arc Magmas

Another isotope system that has contributed significantly to our knowledge of island arc processes is the ^{230}Th-^{238}U system. This system has been important in confirming the role of fluids in arc magma genesis. As we found in Chapter 3, the equilibrium situation is that the activity of ^{230}Th is equal to the activity of ^{238}U, and hence the ratio (^{230}Th/^{232}Th) will be equal to the (^{238}U/^{232}Th) ratio. Equilibrium should characterize the mantle before melting (as well as old sediment). Because Th is more incompatible than U, the (^{238}U/^{232}Th) ratio in a melt should decrease, but the (^{230}Th/^{232}Th) ratio of a melt will be the same as that of its source. Thus on a conventional plot of (^{230}Th/^{232}Th) against (^{238}U/^{232}Th), the melt should be driven to the left of the equiline. As we found in Chapter 6, this is what is observed in MORB and most OIB.

As Figure 7.29 shows, although many arc magmas are close to equilibrium and some do plot to the left of the equiline, many some arcs have (^{238}U/^{232}Th)—(^{230}Th/^{232}Th) values that plot to the right of the equiline, i.e., in arcs, U appears to be going in the melt more readily than Th. The explanation of this is that U is enriched in the peridotitic mantle source of arc magmas by hydrous fluid transport from the lithospheric slab (the sediments and basalts of the oceanic crust). U is fairly soluble in water in its oxidized (6+) form; Th is quite insoluble. Thus hydrous fluids should transport U more readily than Th.

The idea that fluids might be important in transporting material from the slab to the magma genesis zone was proposed on other grounds (the abundance of water in these magmas and the enrichment in

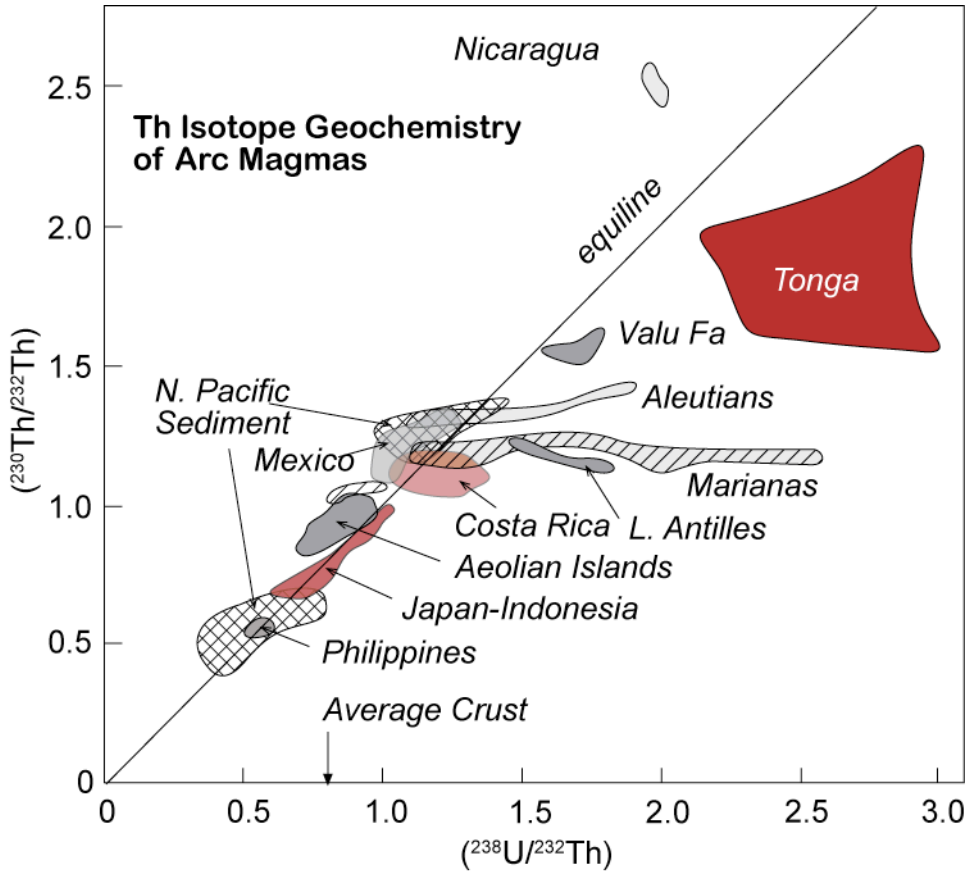

Figure 7.29. (^{230}Th/^{232}Th) vs. (^{238}U/^{232}Th) in island arc magmas. After McDermott and Hawkesworth (1991).

alkalis and alkaline earth trace elements, which are fairly soluble). The Th isotope studies provide confirming evidence of this idea.

7.6 Radiogenic Isotopes in Oceanography

Oceans cover that portion of the Earth's surface not occupied by emergent continental crust and here too radiogenic isotope ratios have proved useful in understanding how the Earth works. In the context of oceanography, we can divide the radiogenic isotopes into two categories: those whose isotopic composition varies in the modern ocean due to their with short residence times in seawater and those whose isotopic composition is uniform in the modern ocean due to their long residence time in seawater. The former include Nd, Hf, and Pb isotope ratios, the latter Sr and, perhaps, Os isotope ratios. In this section, we'll briefly review the use of radiogenic isotopes in oceanography and paleoceanography. A longer and more detailed review can be found in Frank (2002).

7.6.1 Oceanographic Circulation and Geochemical Cycling

Ions enter seawater from a number of sources: rivers, submarine hydrothermal fluids, by diffusion out of sediments, and from dust particles that settle on the ocean surface. Isotopic variations in seawater in time and space can result from both variations in the relative strength of these fluxes and in their isotopic composition. The time required to erase or reduce compositional heterogeneity in the ocean is known as the *mixing time*, and is of the order of 10^3 years. However, this term is neither precisely defined nor precisely known (a reasonable, but not universally used, definition is the time required to reduce compositional variance by a factor of $1/e$). On the other hand, *residence time* in a steady-state system can be precisely defined as the ratio of the mass of an element in the ocean to the flux of that element into (or out of) the ocean. Nd, Hf, and Pb have short residence times not so much because of their insolubility as their particle reactivity: they are readily absorbed onto particles (both organic and inorganic) and removed from solution in this way. The residence time of Nd is in the range of 600-2000 years, that of Hf is estimated at 1500-2000 years, and that of Pb is in the range of 50 to 400 years. Because these elements have residence times similar to or shorter than the mixing time, their isotopic composition varies in the ocean. Sr, on the other hand, has a residence time in the ocean of 2.4 million years and $^{87}Sr/^{86}Sr$ of seawater in the open ocean is uniform at 0.70925, although variations in this value occur in coastal waters. The residence time of Os in seawater is not entirely resolved; it may be as short as a few thousand years or as long as a few tens of thousands of years. The Os isotopic composition of deep ocean water appears to be constant within analytical error, but some variation is observed in surface waters. With the exception of Sr, all these elements are present in seawater at extremely low concentrations (parts per trillion and lower), so these isotopic analyses are extremely challenging.

Ocean circulation is ultimately driven by the pole-to-equator gradient in solar radiative energy or *insolation*. In response to this gradient, the atmosphere and oceans carry heat from low to high latitudes. The surface circulation of the ocean is driven by winds and this, combined with the Coriolis effect, results in paired clockwise and counterclockwise gyres in the northern and southern, respectively, Pacific and Atlantic Oceans. Strong westward flowing equatorial currents occur between these gyres and, particularly in the Pacific, a usually smaller equatorial countercurrent runs eastward. The flow of this countercurrent greatly increases during El Niño events. Indian Ocean circulation has some of these aspects but is more complex and varies seasonally driven by the Indian monsoons.

In contrast, the deep circulation of the ocean is driven by density differences that depend on temperature and salinity. In the modern ocean, temperature has the dominant effect on density so that deep water is "formed", that is acquires its characteristic temperature and salinity, at the high latitude and then flows equatorward at depth. This so-called "Great Conveyor Belt" begins in the North Atlantic, where water cooled in winter in the Norwegian, Greenland and Labrador Seas downwells to become North Atlantic Deep Water (NADW). As it flows south, it entrains Antarctic Bottom Water (AABW) from below and Antarctic Intermediate Water from above and joins the Antarctic Circumpolar Current, which makes it the largest current in the ocean in terms of volume transport, as part of the Circumpolar Deep

Water CDW). Antarctic Bottom Water, the coldest and densest water in the ocean, forms in mainly in the Weddell Sea, during winter when extreme cooling and ice formation increase salinity and decrease temperature. This water then flows northward into all three oceans. The flow is balanced by southward flowing water at shallower depth. Traditionally, these water masses are identified by their temperature and salinity characteristics, which are "conservative" properties of the water mass in that once fixed at the surface, they can change only through mixing with other water masses. These water masses also have unique chemical properties as well, such as dissolved oxygen content, nutrient concentrations and carbon isotope ratios, but these change over time, mainly due to biologic activity. The water masses also acquire unique radiogenic isotope signatures because the isotopic composition of the sources of these elements varies geographically.

To a first approximation, the composition of seawater is "steady-state" which means that the fluxes of ions and other components to seawater are balanced by equal fluxes out of seawater, or *sinks*. For the elements of interest to us here, the primary sinks are absorption on particles, both organic and inorganic, precipitation in manganese nodules on the seafloor (although here again adsorption might be a better description of the actual chemical process), and biological precipitation of calcium carbonate. The latter is the dominant sink for Sr, while the remaining sinks dominate for Nd, Hf, Pb, and Os. While some of these radiogenic tracers are used to document modern ocean circulation, it is the incorporation of these elements into the components of ocean floor sediment that makes them particularly valuable as ocean water tracers because these sedimentary materials provide a historical record how the marine system has changed over time, including both changes in circulation and changes in sources of fluxes of these elements. These changes can then elucidate, among other things, past climate change.

7.6.2 Nd, Hf, Os, and Pb in the modern ocean

As noted above, the greatest usefulness of the radiogenic tracers may be in reconstructing past ocean circulation, i.e., paleoceanography. That, however, requires an understanding of the present distribution of these isotope ratios in the oceans. The first measurements of Nd isotope ratios in seawater were made over thirty years ago (Piepgras and Wasserburg, 1980), so that by now the Nd isotopic composition of seawater, which ranges from ε_{Nd} -27 to 1, is well characterized. Indeed, a database published by Lacan et al. (2012) contain 880 analyses. These are illustrated in Figure 7.30, which shows the frequency distridistribution of ε_{Nd} in the four oceans. The most radiogenic Nd occurs in the Atlantic and Arctic Oceans, with average ε_{Nd} of -11.4±3.4 and -10.1±1.7, respectively. The least radiogenic Nd occurs in the Pacific, with average ε_{Nd} of -3.9±1.8 and the Indian is intermediate, with average ε_{Nd} of -6.6±2.5. Peucker-Ehernbrink et al. (2010) estimate the mean ε_{Nd} of seawater as -7.2±0.5. The radiogenic nature of Pacific Ocean Nd originally suggested hydrothermal inputs might be important (Piepgras and Wasser-

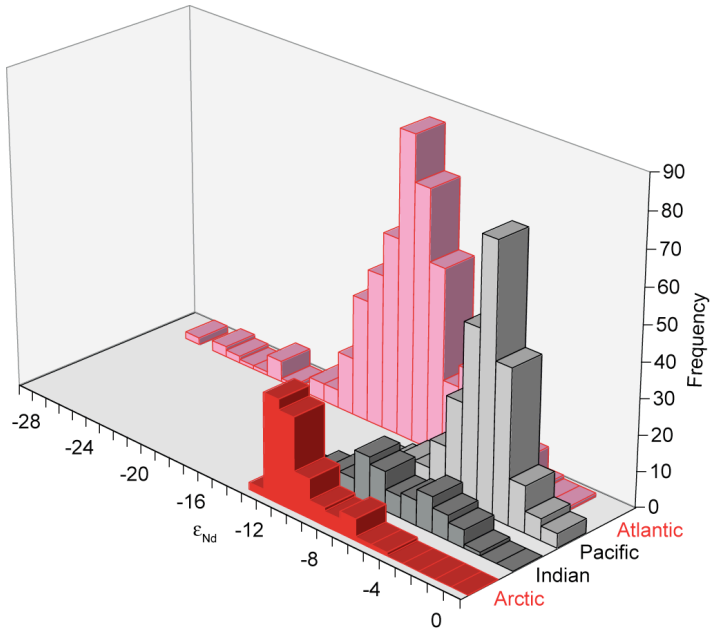

Figure 7.30. Histogram of ε_{Nd} dissolved in seawater, illustrating the radiogenic and unradiogenic nature of Pacific and Atlantic waters, respectively. Atlantic data includes water from the Mediterranean, which is relatively radiogenic. Data from compilation of Lacan et al. (2012).

burg, 1980) because of the greater mid-ocean ridge magmatism and hydrothermal activity there, but subsequent work shows the Nd dissolved in hydrothermal fluids is very quickly scavenged by particles, reducing the hydrothermal input to negligible levels (Halliday et al., 1992). The difference instead relates to the nature and age, and therefore isotopic composition, of geologic provinces supplying Nd to the ocean basins. The Pacific is surrounded by young volcanic arcs with relatively high ε_{Nd} while the Atlantic is surrounded by older tectonic blocks with lower ε_{Nd}, as is well demonstrated in the compilation of Jeandel et al. (2007). The most extremely unradiogenic Nd occurs in the Baffin Bay and the Labrador Sea, which are surrounded by extensive outcropping of Archean crust. Seawater in this region is a major source of NADW, which accounts for the particularly unradiogenic character of this water mass ($\varepsilon_{Nd} \approx -14$). The unradiogenic nature of NADW is somewhat moderated as it flows southward, but it remains distinctive in the extreme South Atlantic where it mixes with Antarctic waters to become part of the CDW with ε_{Nd} of -8 to -9 (Stichel et al., 2012). Waters in the North Pacific tend to have the most radiogenic Nd. Surface waters show greater variability than deep water. Attempts to reproduce the global pattern of ε_{Nd} in the oceans suggest that isotopic exchange between dissolved Nd and Nd in sedimentary particles on continental margins exerts an important control on isotopic composition (e.g., Albarede et al., 1997; Van der Flerdt et al., 2004, Arsouze et al., 2009).

There are far fewer data on Hf isotopic composition as it has only recently become possible to directly measure Hf isotope ratios in seawater (e.g., Zimmermann et al, 2009; Godfrey et al., 2009). Measured values in Atlantic, Arctic and Pacific seawater ranges from ε_{Hf} -5.7 to 8.6. Figure 7.31 shows the relationship between ε_{Hf} and ε_{Nd} in seawater. The data fall along a distinctively lower slope than the terrestrial array (Figure 2.20), and mirror the slope observed in marine sediments and manganese nodules (White et al., 1986; Vervoort et al., 2011), which Albarède et al., (1998) termed the "seawater array". As recognized early on, the discordance between the mantle and seawater arrays results from the difference in behavior of Nd and Hf in weathering (Patchett et al., 2004; White et al., 1986). Whereas Nd concentrates largely in clays and other fine-grained material, much of the budget of Hf in sedimentary rocks is in zircon. Hf in zircon is very unradiogenic due to very low Lu/Hf. Zircon is a heavy mineral that resists mechanical weathering and transport, thus much of it remains in coarse-grained sediments of the continents and continental shelves. Clays and fine-grained accessory minerals, rich in Nd and radiogenic Hf, are more readily transported, by a combination of rivers, currents, and winds, to the deep ocean. This incongruent release of Hf appears to extend to Saharan dust carried to the Atlantic, as while Nd isotopic composition of surface waters is similar to that of dust, the Hf in surface waters is more radiogenic than the dust (Rickli et al, 2010). Hf isotope ratios appear to be less sensitive to ocean circulation changes, limiting the utility of ε_{Hf} as a stand-alone oceanographic tracer (van der Flierdt et al., 2004).

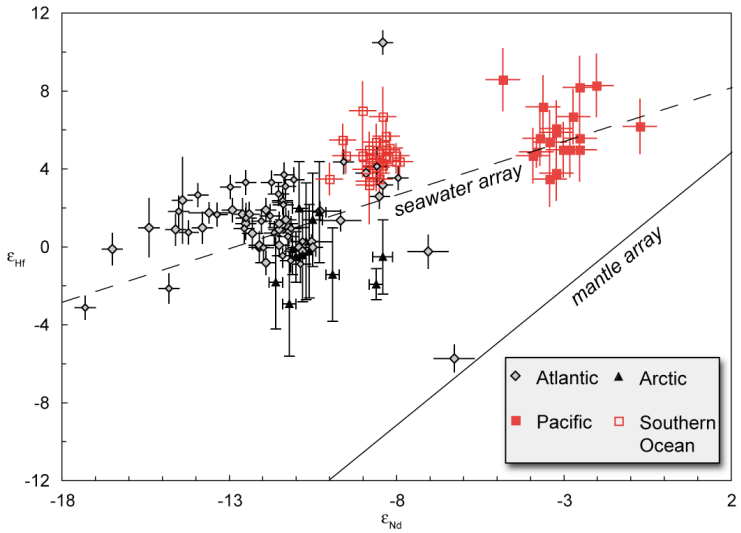

Figure 7.31. ε_{Hf} vs. ε_{Nd} in seawater. The "mantle array" is the correlation in mantle-derived rocks shown in Figure 2.20. The seawater array mirrors that observed in authigenic marine sediments (Vervoort et al., 2011). Data from Godfrey et al., (2009), Zimmermann et al. (2009a, 2009b), Rickli et al. (2009, 2010) and Stichel et al. (2012).

The data also suggest two other differences between Hf and Nd in seawater. First, reduced variance in

Hf isotopic composition is consistent with the longer residence time of Hf in seawater noted in the previous section. Second, the more radiogenic character of Hf, even at the high ε_{Hf}–ε_{Nd} end of the array suggests a greater proportion of 'mantle' in seawater Hf supplied by ridge crest hydrothermal activity (White et al., 1986). Hf is present in river and ocean water mainly as $Hf(OH)_4^-$ and as such is probably present primarily in colloids rather than in truly dissolved form. This colloidal Hf and Zr in river water is removed as the colloids aggregate and settle into the sediment and become during estuarine mixing (Bau and Koschinsky (2006). Thus the radiogenic nature of Hf in seawater may reflect the very low flux of Hf from the continents rather than a particularly high flux from hydrothermal vents.

Pb isotope ratios present perhaps the greatest analytical challenge, because of the extremely low concentrations combined high blank levels that result from with anthropogenic lead. Consequently, relatively few data exist and are reported as $^{207}Pb/^{206}Pb$ and $^{208}Pb/^{206}Pb$ ratios as ^{204}Pb levels are too low to measure accurately. The data that do exist show that even in deep Pacific water, the remotest and oldest seawater, anthropogenic lead dominates (Wu et al., 2010). Data on the natural Pb distribution in the ocean comes largely from manganese nodules on the seafloor, into which seawater Pb is incorporated at high concentration. These data show $^{206}Pb/^{204}Pb$ ratios varying from about 18.5 to 19.3 (von Blanckenburg et al., 1996). As with Nd and Hf, the more "mantle-like" isotopic signatures are found in Pacific Ocean while more radiogenic, crustal-like signatures occur in the Atlantic, particularly the North Atlantic. Pb isotopes are well mixed in the Pacific and there is no evidence for the import of North Atlantic deep water-derived lead into either the Pacific or North Indian Ocean, a consequence of the short residence time of Pb in deep water (80- 100 a). Rivers appear to be the major source of dissolved Pb in seawater, although dissolution of eolian particulates may about for about 12% of the total flux and locally more (Henderson and Maier-Reimer, 2002). Although hydrothermal fluids are Pb-rich, they do not seem to be a significant source of seawater Pb as the Pb is quickly removed by particles in the fluid.

Osmium is, of course, an extremely rare element and this is certainly true in seawater, where the concentration is ~10^{-8} ppm (10^{-14} g/g or 5 x 10^{-14} mol/kg). Osmium isotopic composition of deep water appears to be homogeneous within analytical error at $^{187}Os/^{188}Os = 1.067 \pm 0.011$ (Sharma et al., 1997; Levasseur et al., 1998; Woodhouse et al., 1999), which reflects a balance of a variety of sources. Interestingly, interplanetary dust particles and meteorites are a small but significant (5%) source of seawater. That source and hydrothermal systems developed on abyssal peridotite provide unradiogenic Os ($^{187}Os/^{188}Os \approx 0.13$) to balance radiogenic Os from the continents (e.g., Burton et al., 2010), which has an average $^{187}Os/^{188}Os$ of 1.4. Most of this continental Os is provided by rivers, but the eolian flux is difficult to evaluate since loess has the same $^{187}Os/^{188}Os$ as seawater (Peucker-Ehrenbrink and Jahn, 2001). Chen et al. (2009) have reported $^{187}Os/^{188}Os$ ratios as low as 0.76 in Atlantic surface waters, which the authors interpret as reflecting recent anthropogenic inputs.

7.6.3 Radiogenic Isotopes in Paleoceanography

Neodymium isotope ratios have found particularly widespread use in studying ocean circulation changes associated with the climatic oscillations of the Pleistocene. As we'll discuss in Chapter 10, the "Ice Ages" resulted from small variations in the Earth's orbit and rotation (the Milankovitch variations) that changed the amount of solar energy, or insolation, that reached high northern latitudes. This triggered a number of other changes that greatly amplified the small insolation signal into quite large changes in global climate. One of the most important of these amplifying factors was changes in ocean circulation, particularly in the North Atlantic and in production of North Atlantic Deep Water (NADW). As we found in the previous section, NADW has a uniquely unradiogenic Nd isotope signature of NADW, which can be imprinted on to the various authigenic components of ocean floor sediment, most notably ferromanganese nodules, crusts, and coatings on detrital and biogenic particles as the water mass flows southward. The latter can be selectively removed from the sediment by leaching with a complexing agent such as hydroxylamine hydrochloride or ethylenediaminetetraacetic acid (EDTA) and a stratigraphic history of the Nd isotopic composition of bottom water reconstructed. Figure 7.32 shows Nd isotopic variations of bottom water determined in this way from two localities, the

Blake Ridge, off the coast of the southeastern US, and the Cape Basin, southeast of the Cape of Good Hope. The longer Cape Basin record (Piotrowski et al., 2005, 2008) shows irregular variations through the Wisconsinan Ice Age that can be correlated with climatic and oceanographic events documented from sedimentological and stable isotope studies (we'll discuss these in Chapter 10). Both records exhibit a decrease in ε_{Nd} as the Wisconsinan ended, indicating a change to a circulation pattern similar to the present with a strong flow of NADW as ice volumes decreased (compare Figure 10.19). The NADW signal is stronger in the Blake Plateau record (Guthjahr et al., 2008, 2010) because, unlike in the Cape Basin, it is relatively undiluted with southern ocean waters.

Because lead has three radiogenic isotopes, it can be possible to indentify multiple causative factors in isotope ratios variations. In the modern ocean, relatively warm (~10˚C) but highly saline and therefore dense water flowing out of the Strait of Gibraltar plays and important role in North Atlantic circulation and, ultimately, in production of NADW. Some of this Mediterranean Outflow water (MOW) spreads out in the Central Atlantic at a depth of about 1000 m forming so-called Mediterranean Intermediate Water (MIW), while part of it flows north along the eastern Atlantic margin toward the Norwegian-Greenland Sea where its highly saline character preconditions NADW formation. Stichel et al. (2010) analyzed Nd and Pb isotope ratios in authigenic components of sediments of the Iberian continental margin. The Nd isotope ratios were compromised, probably by exchange with sediments carried downslope in the nepheloid layer, but Pb isotope revealed changes in both the isotopic composition of MOW and its outflow pattern over the last 23,000 years. Isotopic composition changes of the MOW were likely due to changing balances of riverine and eolian Pb input to the Mediterranean; glacial climates were drier and likely favored a greater eolian input. Changes in outflow pattern could be linked to changes in NADW production discussed above.

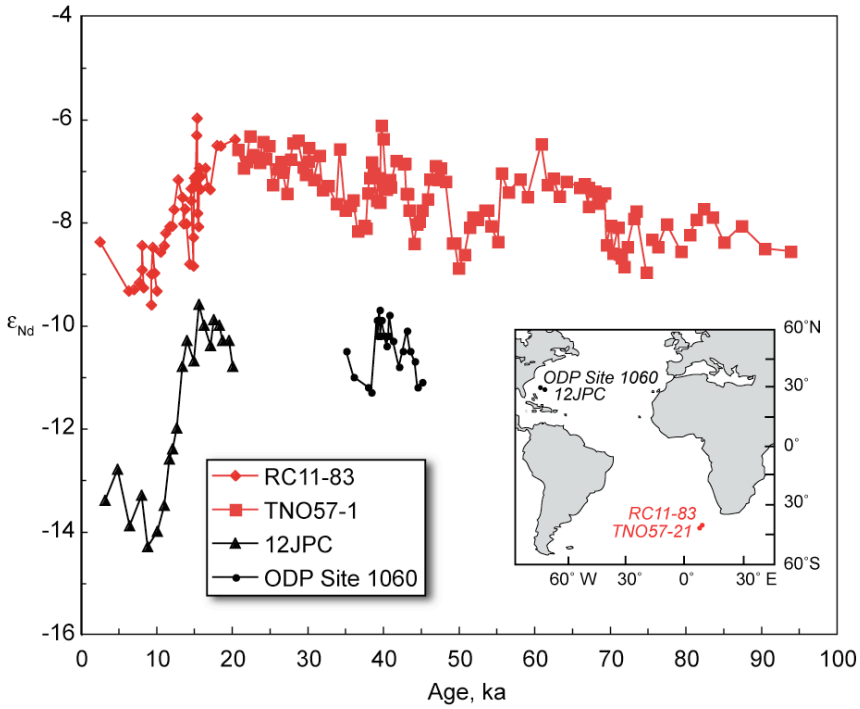

Figure 7.32. Variation in Nd isotopic composition of bottom water at two localities (locations shown in inset) as recorded by ferromanganese coatings on sedimentary particles in 4 cores. Data from Piotrowski et al., (2005), Gutjahr et al., (2008) and Gutjahr et al. (2010).

On longer time scales, both Nd and Pb isotope ratios in manganese crusts suggest the present deep circulation of the Atlantic, and the characteristic radiogenic Pb and unradiogenic Nd of deep water, has only been established within the last 8 Ma (O'Nions et al., 1998). The cause of the isotopic shift is unclear. Smaller shifts in ε_{Nd} are observed in the Pacific around 3 to 5 Ma, which corresponds to the closure of the Isthmus of Panama. O'Nions et al. (1998) speculate this may reflect the flow of NADW into the Pacific. The relatively unradiogenic nature of Pb in the North Pacific seems to have been maintained throughout the Cenozoic (Chen et al., 2013).

Chapter 7 The Continental Crust & Oceans

As we pointed out in Chapter 2, the Os isotopic composition of seawater has varied through time as a consequence of variation in the proportion of crustal, mantle and crustal fluxes to seawater. As Figure 7.33 shows, there has been a particularly rapid increase in $^{187}Os/^{188}Os$, similar to that observed for $^{87}Sr/^{86}Sr$ (Figure 2.12). The likely cause of both is an increase of continental weathering flux resulting from Cenozoic mountain-building, most notably the rise of Himalaya, but also the Alps, Rockies, and Andes (Peucker-Ehrenbrink et al., 1995). It may also reflect a decreasing hydrothermal flux resulting from decreasing sea floor spreading rates. The geochemical behavior of both at the surface of the Earth is related to carbon, but while Sr is concentrated in carbonates, Os is concentrated in organic rich sediments.

Very low $^{87}Os/^{188}Os$ occurs exactly at the Cretaceous-Tertiary boundary (65.5 Ma). The inset shows a high-resolution study of the Gubbio Formation in Italy by Robinson et al. (2009). The lowest ratios occur right at the Cretaceous-Tertiary Boundary and are associated with elevated Ir, Os, and Pt concentrations, and are thus almost certainly due to a chondritic Os ($^{187}Os/^{188}Os = 0.128$) delivered by the Chicxulub impactor. The study shows, however, that $^{187}Os/^{188}Os$ began to decline more than 500,000 years before the K-T boundary and similar declines are observed in several ODP cores. One possibility is that diagenetic remobilization has smeared out the impactor signal, but based on platinum group element concentrations, Robinson et al. concluded that in the Gubbio this affects $^{187}Os/^{188}Os$ no more than a meter (corresponding to roughly 70,000 years) from the boundary. The authors conclude the decline was a consequence of Deccan volcanism, although it is unclear whether the decline is a result of mantle Os released by Deccan volcanism or some indirect cause.

Osmium isotopes also show shorter-term variations reflecting the changing balance of crustal, cosmic, and mantle fluxes. Figure 7.34 shows the $^{187}Os/^{188}Os$ in cleaned foraminifera in sediment from ODP Site 578 in the Indian Ocean (Burton et al., 2010) and in bulk sediment in two cores from the southeastern Pacific (Oxburgh, 1998). Overall, there is good agreement between the two, though the Indian Ocean data show more variation, perhaps because of a component of detrital sediment in the Pacific cores, whereas foraminiferal calcite should contain only seawater-derived Os. Both data sets show minima at the last glacial maximum, approximately 20,000 years ago, and the previous one, approximately 150,000 to 160,000 years ago. Variations likely result from a decrease in the delivery of high $^{187}Os/^{186}Os$ continental weathering products to the ocean in the drier glacial climate. The $^{187}Os/^{186}Os$ also strongly, but not perfectly, anti-correlate with ε_{Nd} measured in foraminifera from Site 578 by Burton and Vance (2000). The previous glacial maximum in ε_{Nd} (note the scale is inverted) occurs somewhat later, around 135,000 years ago, than the $^{187}Os/^{186}Os$ minimum. Both Oxburgh (1998) and Burton et al. (2010) argue that the data are consistent with residence time (<12,000 years) that is

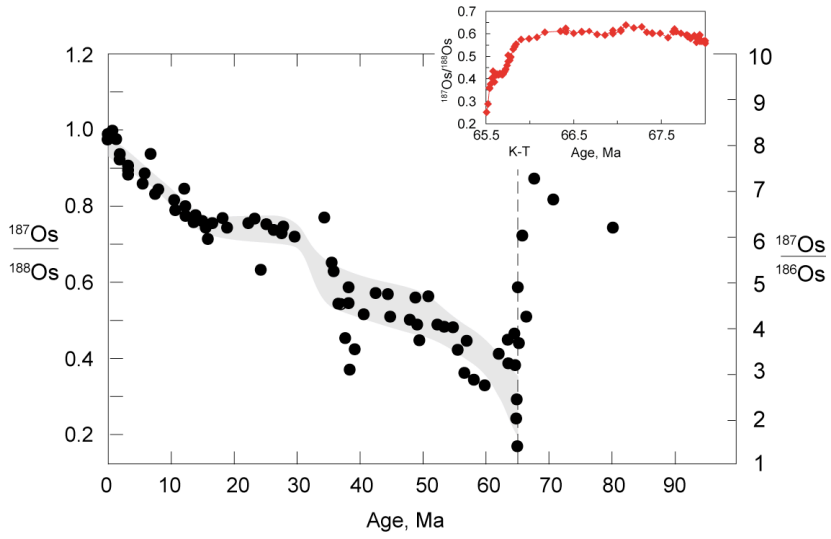

Figure 7.33. Os isotope composition of seawater over the last 80 Ma based on data in Peucker-Ehrenbrink et al. (1995) and Peucker-Ehrenbrink and Ravizza (2000). Gray field represents Peucker-Ehrenbrink et al.'s (1995) best estimates of seawater Os isotopic composition. Inset show the data from the late Cretaceous Gubbio Formation of Robinson et al., (2009). K-T is the Cretaceous-Tertiary Boundary.

closer to the short end of the range of estimates (4000 to 40,000 years).

As Figure 2.12 shows, the $^{87}Sr/^{86}Sr$ of seawater has increased dramatically through the Cenozoic from about 0.7078 to 0.70925 at present. This changing isotopic composition results from changes in either the hydrothermal Sr flux, the riverine Sr flux or the $^{87}Sr/^{86}Sr$ of the riverine flux or some combination of these. Richter et al. (1992) argued that the changes are too great to be explained by the hydrothermal flux and that the most likely explanation relates to the rise of the Himalayas. In support of that hypothesis, they noted that the most rapid change in seawater $^{87}Sr/^{86}Sr$ occurred between 15 and 20 Ma, a time of exceptionally high erosion rates in the Himalaya. Sr in rivers draining the Himalaya is also exceptionally radiogenic. The Ganges, for example, has a $^{87}Sr/^{86}Sr$ of 0.725 while that of the Brahmaputra is 0.720 compared to a global average riverine $^{87}Sr/^{86}Sr$ of 0.7111 (Peucker-Ehrenbrink et al., 2010).

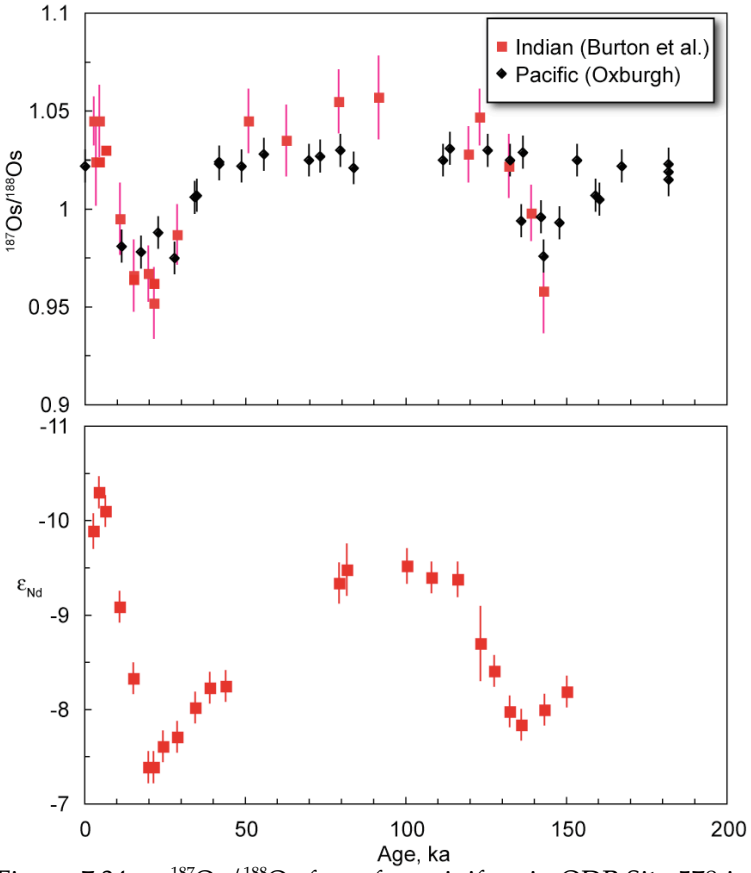

Figure 7.34. a. $^{187}Os/^{188}Os$ from foraminifera in ODP Site 578 in the Indian Ocean (Burton et al., 2010) and bulk sediment in cores V19-54 and V19-55 in the Pacific (Oxburgh, 1998). b. Nd isotope ratios in shells of the foram *G. menardii* from ODP Site 578 (Burton and Vance, 2000).

The long residence time of Sr in the ocean means that its isotopic composition is largely insensitive to variations in fluxes on the time scale of glacial-interglacial fluxes, but variations do occur on the time scales of several hundred thousand years. These shorter-term variations also cannot be accounted by changes in the hydrothermal flux and hence must be due to changes in the riverine flux or its isotopic composition. Capo and DePaolo (1990) noted the correlation between changes in seawater $^{87}Sr/^{86}Sr$ and climate proxies, such as $\delta^{18}O$ (we will discuss these in Chapter 10). Derry and France-Lanord (1996) suggested that in this case the connection between seawater $^{87}Sr/^{86}Sr$ might be the opposite of expected. They argued that reduced erosion rates but increased weathering intensity during the Pliocene released proportionally more Sr minerals with high Rb/Sr like biotite and less from low Rb/Sr minerals such as calcite and plagioclase. The result was a decrease in the Himalaya riverine flux but an increase in its $^{87}Sr/^{86}Sr$ in the Pliocene.

References and Suggestions for Further Reading

Albarède, F., Goldstein, S. L. & Dautel, D. 1997. The neodymium isotopic composition of manganese nodules from the Southern and Indian oceans, the global oceanic neodymium budget, and their bearing on deep ocean circulation. *Geochimica et Cosmochimica Acta*, 61, 1277-1291, doi: 10.1016/S0016-7037(96)00404-8.

Albarède, F., Simonetti, A., Vervoort, J. D., Blichert-Toft, J. & Abouchami, W. 1998. A Hf-Nd isotopic correlation in ferromanganese nodules. *Geophysical Research Letters*, 25, 3895-3898, doi: 10.1029/1998gl900008.

Armstrong, R. L., 1968. A model for the evolution of strontium and lead isotopes in a dynamic Earth. *Reviews of Geophysics*, 6:175-199.

Armstrong, R. L., 1971. Isotopic and chemical constraints on models of magma genesis in volcanic arcs, *Earth and Planetary Science Letters, 12*, 137-142.

Armstrong, R. L., 1981. Radiogenic isotopes: the case for crustal recycling on a near-steady-state no-continental-growth Earth, in S. Moorbath and Windley, B. F. (ed.), *The Origin and Evolution of the Earth's Continental Crust*, 259-287, The Royal Society, London.

Arsouze, T., Dutay, J. C., Lacan, F. & Jeandel, C. 2009. Reconstructing the Nd oceanic cycle using a coupled dynamical–biogeochemical model. *Biogeosciences*, 6, 2829-2846, doi: 10.5194/bg-6-2829-2009.

Asmerom, Y. and S. B. Jacobsen. 1993. The Pb isotopic evolution of the Earth: inferences from river water suspended loads. *Earth and Planetary Science Letters*, 115: 245-256.

Bau, M. & Koschinsky, A. 2006. Hafnium and neodymium isotopes in seawater and in ferromanganese crusts: The "element perspective". *Earth and Planetary Science Letters*, 241, 952-961, doi: 10.1016/j.epsl.2005.09.067.

Ben Othman, D., W. M. White, and J. Patchett, The geochemistry of marine sediments, island arc magma genesis, and crust-mantle recycling, *Earth and Planetary Science Letters*, 94, 1-21, 1989.

Bennett, V. C. and D. J. DePaolo, 1987. Proterozoic crustal history of the western United States as determined by neodymium isotope mapping. *Bulletin of the Geological Society of America*, 99: 674-685.

Bennett, V. C., A. D. Brandon and A. P. Nutman, 2007. Coupled ^{142}Nd-^{143}Nd isotopic evidence for Hadean mantle dynamics, *Science*, 318:1907-1910.

Boyet, M. & Carlson, R. L. 2006. A new geochemical model for the Earth's mantle inferred from 146Sm–^{142}Nd systematics. *Earth and Planetary Science Letters*, 250, 254-268.

Boyet, M. and R. L. Carlson, 2005. ^{142}Nd evidence for early (>4.3 Ga) global differentiation of the silicate Earth, *Science*, 309: 576-581.

Boyet, M., J. Blichert-Toft, M. Rosing, M. Storey, P. Telouk and F. Albarede, 2003. 142Nd evidence for early Earth differentiation, *Earth and Planetary Science Letters*, 214:427-442.

Burton, K. W. & Vance, D. 2000. Glacial–interglacial variations in the neodymium isotope composition of seawater in the Bay of Bengal recorded by planktonic foraminifera. *Earth and Planetary Science Letters*, 176, 425-441, doi: 10.1016/S0012-821X(00)00011-X.

Burton, K. W., Gannoun, A. & Parkinson, I. J. 2010. Climate driven glacial–interglacial variations in the osmium isotope composition of seawater recorded by planktic foraminifera. *Earth and Planetary Science Letters*, 295, 58-68, doi: 10.1016/j.epsl.2010.03.026.

Capo, R. C. & DePaolo, D. J. 1990. Seawater strontium isotopic variations from 2.5 million years ago to the present. *Science*, 249, 51-55.

Caro, G., B. Bourdon, J.-L. Birck and S. Moorbath, ^{146}Sm-^{142}Nd evidence from Isua metamorphosed sediments for early differentiation of the Earth's mantle, *Nature*, 423: 428-432, 2003.

Carpentier, M., C. Chauvel and N. Mattielli, 2008. Pb-Nd isotopic constraints on sedimentary input into the Lesser Antilles arc system, *Earth and Planetary Science Letters*, 272:199-211.

Cates, N. L., Ziegler, K., Schmitt, A. K. & Mojzsis, S. J. 2013. Reduced, reused and recycled: Detrital zircons define a maximum age for the Eoarchean (ca. 3750-3780 Ma) Nuvvuagittuq Supracrustal Belt, Québec (Canada). *Earth and Planetary Science Letters*, 362, 283-293, doi: 10.1016/j.epsl.2012.11.054.

Chappell, B. W. and A. White, Two contrasting granite types, Pac. Geol., 8:173-174,1974.

Chen, C., Sedwick, P. N. & Sharma, M. 2009. Anthropogenic osmium in rain and snow reveals global-scale atmospheric contamination. *Proceedings of the National Academy of Sciences*, 106, 7724-7728, doi: 10.1073/pnas.0811803106.

Chen, T.-Y., Ling, H.-F., Hu, R., Frank, M. & Jiang, S.-Y. 2013. Lead isotope provinciality of central North Pacific Deep Water over the Cenozoic. *Geochemistry, Geophysics, Geosystems*, 14, 1523-1537, doi:10.1002/ggge.20114.

Chou, C.-L. 1978. Fractionation of siderphile elements in the Earth's upper mantle and lunar samples. Proceedings of the Lunar and Planetary Science Conference, 9, 163-165.

Compston, W. and R. T. Pidgeon, Jack Hills, 1986. evidence of more very old detrital zircons in Western Australia, Nature, 321:766-769.

Condie, K. C. 1995, Episodic ages of greenstones: a key to mantle dynamics? *Geophysical Research Letters*, 22:2215-2218.

Condie, K. C., Episodic continental growth and supercontinents: a mantle avalanche connection? *Earth and Planetary Science Letters*, 163:97-108,10.1016/s0012-821x(98)00178-2 1998.

Davies, G. F., 1984. Geophysical and isotopic constraints on mantle convection: An interim synthesis., *Journal of Geophysical Research, 89*, 6017-6040, 1984.

Debaille, V., O'Neill, C., Brandon, A. D., Haenecour, P., Yin, Q.-Z., Mattielli, N. & Treiman, A. H. 2013. Stagnant-lid tectonics in early Earth revealed by ^{142}Nd variations in late Archean rocks. *Earth and Planetary Science Letters*, 373, 83-92, doi: 10.1016/j.epsl.2013.04.016.

Derry, L. A. & France-Lanord, C. 1996. Neogene Himalayan weathering history and river ^{87}Sr/^{86}Sr: impact on the marine Sr record. *Earth and Planetary Science Letters*, 142, 59-74.

Edmond, J. M. 1992. Himalayan tectonics, weathering processes, and the strontium isotope record in marine limestones. *Science*. 258: 1594-1597.

Esser, B. K. and K. K. Turekian. 1993. The osmium isotopic composition of the continental crust. *Geochimica et Cosmochimica Acta*. 57: 3093-3104.

Faure, G. 1986. *Principles of Isotope Geology*. New York: Wiley & Sons.

Frank, M. 2002. Radiogenic isotopes: tracers of past ocean circulation and erosional input. *Reviews of Geophysics*, 40, 1-1-1-38, doi: 10.1029/2000rg000094.

Froude, D.O., Ireland, T.R., Kinny, P.D., Williams, I.S., Compston, W., Williams, I.R., and Myers, J.S., 1983. Ion microprobe identification of 4100-4200 Myr-old terrestrial zircons. *1984*. 304, 616–618.

Garçon, M., Chauvel, C., France-Lanord, C., Limonta, M. & Garzanti, E. 2013. Removing the "heavy mineral effect" to obtain a new Pb isotopic value for the upper crust. *Geochemistry, Geophysics, Geosystems*, 14, doi:10.1002/ggge.20219.

Godfrey, L. V., Zimmermann, B., Lee, D. C., King, R. L., Vervoort, J. D., Sherrell, R. M. & Halliday, A. N. 2009. Hafnium and neodymium isotope variations in NE Atlantic seawater. *Geochemistry, Geophysics, Geosystems*, 10, Q08015, doi: 10.1029/2009gc002508.

Goldstein, S. J. and S. B. Jacobsen. 1987. The Nd and Sr isotopic systematics of river-water dissolved material: implications for the sources of Nd and Sr in seawater. *Chem. Geol. (Isot. Geosci. Sect.)*. 66: 245-272.

Goldstein, S. J. and S. B. Jacobsen. 1988. Nd and Sr isotopic systematics of river-water suspended material: implications for crustal evolution. *Earth and Planetary Science Letters*, 87: 249-265.

Goldstein, S. L., R. K. O,Nions, and P. J. Hamilton, 1986. A Sm-Nd study of atmospheric dusts and particulates from major river systems, *Earth and Planetary Science Letters*, 70, 221-236.

Gutjahr, M., Frank, M., Stirling, C. H., Keigwin, L. D. & Halliday, A. N. 2008. Tracing the Nd isotope evolution of North Atlantic Deep and Intermediate Waters in the western North Atlantic since the Last Glacial Maximum from Blake Ridge sediments. *Earth and Planetary Science Letters*, 266, 61-77, doi: 10.1016/j.epsl.2007.10.037.

Gutjahr, M., Hoogakker, B. A. A., Frank, M. & McCave, I. N. 2010. Changes in North Atlantic Deep Water strength and bottom water masses during Marine Isotope Stage 3 (45–35 ka BP). *Quaternary Science Reviews*, 29, 2451-2461, doi: 10.1016/j.quascirev.2010.02.024.

Halliday, A. N., 2004. Mixing, volatile loss and compositional change during impact-drive accretion of the Earth, Nature, 427:505-509.

Harrison, T. M., J. Blichert-Toft, W. Muller, F. Albarede, P. Holden and S. J. Mojzsis, Heterogeneous Hadean hafnium: evidence of continental crust at 4.4 to 4.5 Ga, *Science*, 310:1947-1950, 2005.

Hawkesworth, C. J. & Kemp, A. I. S. 2006. Using hafnium and oxygen isotopes in zircons to unravel the record of crustal evolution. *Chemical Geology*, 226, 144-162.

Hawkesworth, C. J., Dhuime, B., Pietranik, A. B., Cawood, P. A., Kemp, A. I. S. & Storey, C. D. 2010. The generation and evolution of the continental crust. *Journal of the Geological Society*, 167, 229-248, doi:10.1144/0016-76492009-072.

Henderson, G. M. & Maier-Reimer, E. 2002. Advection and removal of ^{210}Pb and stable Pb isotopes in the oceans: a general circulation model study. *Geochimica et Cosmochimica Acta*, 66, 257-272, doi: 10.1016/S0016-7037(01)00779-7.

Huang, Y., Chubakov, V., Mantovani, F., Rudnick, R. L. & McDonough, W. F. 2013. A reference Earth model for the heat-producing elements and associated geoneutrino flux. *Geochemistry, Geophysics, Geosystems*, 14, 2003-2029, doi: 10.1002/ggge.20129.

Hurley, P, M., H. Hughes, G. Faure, H. W. Fairbairn, and W. H. Pinson, Radiogenic strontium-87 model of continent formation, *J. Geophys. Res.*, 67, 5315-5334, 1962.

Hurley, P. M., and J. R. Rand, Pre-drift continental nuclei, *Science*, 164, 1229-1242, 1969.

Iizuka, T., Horie, K., Komiya, T., Maruyama, S., Hirata, T., Hidaka, H. & Windley, B. F. 2006. 4.2 Ga zircon xenocryst in an Acasta gneiss from northwestern Canada: Evidence for early continental crust. *Geology*, 34, 245-248, doi:10.1130/g22124.1.

Jackson, M. G. & Carlson, R. W. 2012. Homogeneous superchondritic ^{142}Nd/^{144}Nd in the mid-ocean ridge basalt and ocean island basalt mantle. *Geochemistry, Geophysics, Geosystems*, 13, Q06011, doi:10.1029/2012gc004114.

Kemp, A. I. S., S. A. Wilde, C. J. Hawkesworth, C. D. Coath, A. Nemchin, R. T. Pidgeon, J. D. Vervoort and S. A. DuFrane, Hadean crustal evolution revisited: New constraints from Pb-Hf isotope systematics of the Jack Hills zircons, *Earth and Planetary Science Letters*, 296:45-56,10.1016/j.epsl.2010.04.043 2010.

Lacan, F., Tachikawa, K. & Jeandel, C. 2012. Neodymium isotopic composition of the oceans: A compilation of seawater data. *Chemical Geology*, 300-301, 177-184, doi 10.1016/j.chemgeo.2012.01.019.

Levasseur, S., Birck, J.-L. & Allègre, C. J. 1998. Direct measurement of femtomoles of osmium and the ^{187}Os/^{186}Os ratio in seawater. *Science*, 282, 272-274, doi:10.1126/science.282.5387.272.

McDermott, F., and C. Hawkesworth, 1991. Th, Pb, and Sr isotope variations in young island arc volcanics and oceanic sediments, *Earth and Planetary Science Letters, 104*, 1-15, doi: 10.1016/0012-821X(91)90232-7.

Newsom, H. E., W. M. White, K. P. Jochum, and A. W. Hofmann, Siderophile and chalcophile element abundances in oceanic basalts, Pb isotope evolution and growth of the Earth's core, *Earth and Planetary Science Letters, 80*, 299-313, 1986.

O'Neil, J., Carlson, R. W., Paquette, J.-L. & Francis, D. 2012. Formation age and metamorphic history of the Nuvvuagittuq Greenstone Belt. *Precambrian Research*, 220-221, 23-44, doi: 10.1016/j.precamres.2012.07.009.

O'Niel, J., R. L. Carlson, D. Francis and R. K. Stevenson, Neodymium-142 evidence for Hadean mafic crust, Science, 321:1828-1831, 2008.

O'Nions, R. K., Frank, M., von Blanckenburg, F. & Ling, H. F. 1998. Secular variation of Nd and Pb isotopes in ferromanganese crusts from the Atlantic, Indian and Pacific Oceans. *Earth and Planetary Science Letters*, 155, 15-28, doi: 10.1016/S0012-821X(97)00207-0.

Oxburgh, R. 1998. Variations in the osmium isotope composition of sea water over the past 200,000 years. *Earth and Planetary Science Letters*, 159, 183-191, doi: 10.1016/S0012-821X(98)00057-0.

Palmer, M. R. and J. M. Edmond. 1989. The strontium isotope budget of the modern ocean. *Earth and Planetary Science Letters*, 92: 11-26.

Patchett, P. J., White, W. M., Feldmann, H., Kielinczuk, S. & Hofmann, A. W. 1984. Hafnium/rare earth element fractionation in the sedimentary system and crustal recycling into the Earth's mantle. *Earth and Planetary Science Letters*, 69, 365-378.

Paul, D., W. M. White and D. L. Turcotte, 2003. Constraints on the $^{232}Th/^{238}U$ ratio (κ) of the continental crust, *Geochemistry Geophysics Geosystems*, 4, doi: 10.1029/2002GC000497.

Pegram, W. J., B. K. Esser, S. Krishnaswami and K. K. Turekian. 1994. The isotopic composition of leachable osmium from river sediments. *Earth and Planetary Science Letters*. 128: 591-599.

Peucker-Ehrenbrink, B. & Ravizza, G. 2000. The marine osmium isotope record. *Terra Nova*, 12, 205-219, doi: 10.1046/j.1365-3121.2000.00295.x.

Peucker-Ehrenbrink, B., G. Ravissa and A. W. Hoffmann. 1995. The marine $^{187}Os/^{186}Os$ record of the past 80 million years. *Earth and Planetary Science Letters* 130: 155-167.

Peucker-Ehrenbrink, B., Miller, M. W., Arsouze, T. & Jeandel, C. 2010. Continental bedrock and riverine fluxes of strontium and neodymium isotopes to the oceans. *Geochemistry, Geophysics, Geosystems*, 11, Q03016, doi:10.1029/2009gc002869.

Piepgras, D. J. & Wasserburg, G. J. 1980. Neodymium isotopic variations in seawater. *Earth and Planetary Science Letters*, 50, 128-138, doi: 10.1016/0012-821X(80)90124-7.

Piotrowski, A. M., Goldstein, S. L., Hemming, S. R. & Fairbanks, R. G. 2005. Temporal Relationships of Carbon Cycling and Ocean Circulation at Glacial Boundaries. *Science*, 307, 1933-1938, doi: 10.1126/science.1104883.

Piotrowski, A. M., Goldstein, S. L., R, H. S., Fairbanks, R. G. & Zylberberg, D. R. 2008. Oscillating glacial northern and southern deep water formation from combined neodymium and carbon isotopes. *Earth and Planetary Science Letters*, 272, 394-405, doi: 10.1016/j.epsl.2008.05.011.

Richter, F. M., Rowley, D. B. & DePaolo, D. J. 1992. Sr isotope evolution of seawater: the role of tectonics. *Earth and Planetary Science Letters*, 109, 11-23.

Rickli, J., Frank, M. & Halliday, A. N. 2009. The hafnium-neodymium isotopic composition of Atlantic seawater. *Earth and Planetary Science Letters*, 280, 118-127, doi: 10.1016/j.epsl.2009.01.026.

Rickli, J., Frank, M., Baker, A. R., Aciego, S., de Souza, G., Georg, R. B. & Halliday, A. N. 2010. Hafnium and neodymium isotopes in surface waters of the eastern Atlantic Ocean: Implications for sources and inputs of trace metals to the ocean. *Geochimica et Cosmochimica Acta*, 74, 540-557, doi: 10.1016/j.gca.2009.10.006.

Rizo, H., Boyet, M., Blichert-Toft, J. & Rosing, M. T. 2013. Early mantle dynamics inferred from ^{142}Nd variations in Archean rocks from southwest Greenland. *Earth and Planetary Science Letters*, 377–378, 324-335, doi: 10.1016/j.epsl.2013.07.012.

Rizo, H., Boyet, M., Blichert-Toft, J., O'Neil, J., Rosing, M. T. & Paquette, J.-L. 2012. The elusive Hadean enriched reservoir revealed by ^{142}Nd deficits in Isua Archaean rocks. *Nature*, 491, 96-100, doi: 10.1038/nature11565.

Robinson, N., Ravizza, G., Coccioni, R., Peucker-Ehrenbrink, B. & Norris, R. 2009. A high-resolution marine $^{187}Os/^{188}Os$ record for the late Maastrichtian: Distinguishing the chemical fingerprints of Deccan volcanism and the KP impact event. *Earth and Planetary Science Letters*, 281, 159-168, doi: 10.1016/j.epsl.2009.02.019.

Roth, A. S. G., Bourdon, B., Mojzsis, S. J., Touboul, M., Sprung, P., Guitreau, M. & Blichert-Toft, J. 2013. Inherited ^{142}Nd anomalies in Eoarchean protoliths. *Earth and Planetary Science Letters*, 361, 50-57, doi: 10.1016/j.epsl.2012.11.023.

Rudnick, R. L. and D. M. Fountain, Nature and composition of the continental crust: a lower crustal perspective, *Rev. Geophys.*, 33:267-309, 1995.

Rudnick, R. L., and S. L. Goldstein, 1990. The Pb isotopic compositions of lower crustal xenoliths and the evolution of lower crustal Pb, *Earth and Planetary Science Letters, 98*, 192-207, doi: 10.1016/0012-821X(90)90059-7.

Rudnick, R. L., Xenoliths — samples of the lower crust, in *Continental Lower Crust*, edited by D. M. Fountain, R. Arculus, and R. W. Kay, 1992. 269-316 pp., Elsevier, Amsterdam.

Scholl, D. W. & von Huene, R. 2009. Implications of estimated magmatic additions and recycling losses at the subduction zones of accretionary (non-collisional) and collisional (suturing) orogens. *Geological Society of London Special Publications*, 318, 105-125, doi:10.1144/sp318.4.

Sharma, M., Papanastassiou, D. A. & Wasserburg, G. J. 1997. The concentration and isotopic composition of osmium in the oceans. *Geochimica et Cosmochimica Acta*, 61, 3287-3299, doi: 10.1016/S0016-7037(97)00210-X.

Stichel, T., Frank, M., Rickli, J. r. & Haley, B. A. 2012. The hafnium and neodymium isotope composition of seawater in the Atlantic sector of the Southern Ocean. *Earth and Planetary Science Letters*, 317–318, 282-294, doi: 10.1016/j.epsl.2011.11.025.

Stumpf, R., Frank, M., Schönfeld, J. & Haley, B. A. 2010. Late Quaternary variability of Mediterranean Outflow Water from radiogenic Nd and Pb isotopes. *Quaternary Science Reviews*, 29, 2462-2472, doi: 10.1016/j.quascirev.2010.06.021.

Taylor, S. R. and S. M. McLennan, *The continental crust: its composition and evolution*, Oxford, Blackwell Scientific Publications, 312, 1985.

Taylor, S. R. and S. M. McLennan, The geochemical evolution of the continental crust, *Reviews of Geophysics*, 33:241-265, 1995.

Tera, F., L. Brown, J. D. Morris, I. S. Sacks, J. Klein and R. Middleton, Sediment incorporation in island-arc magmas: Inferences from ^{10}Be, *Geochimica et Cosmochimica Acta*, 50:535-550,1986.

Touboul, M., Puchtel, I. S. & Walker, R. J. 2012. ^{182}W evidence for long-term preservation of early mantle differentiation products. *Science*, 335, 1065-1069, doi:10.1126/science.1216351.

Touboul, M., Puchtel, I. S. & Walker, R. J. 2013. Tungsten isotope heterogeneities in Archean komatiites. *Mineralogical Magazine*, 77, 2348.

Upadhyay, D., Scherer, E. E. & Mezger, K. 2009. ^{142}Nd evidence for an enriched Hadean reservoir in cratonic roots. *Nature*, 459, 1118-1121, doi: 10.1038/nature08089.

van de Flierdt, T., Frank, M., Lee, D.-C., Halliday, A. N., Reynolds, B. C. & Hein, J. R. 2004. New constraints on the sources and behavior of neodymium and hafnium in seawater from Pacific Ocean ferromanganese crusts. *Geochimica et Cosmochimica Acta*, 68, 3827-3843, doi: 10.1016/j.gca.2004.03.009.

Vervoort, J. D., Fisher, C. M. & Kemp, A. I. S. 2013. The myth of a highly heterogeneous Hf-Nd Eoarchean mantle and large early crustal volumes. *Mineralogical Magazine*, 77, 2409,

Vervoort, J. D., P. J. Patchett, G. E. Gehrels and A. P. Nutmann. 1996. Constraints on early differentiation from hafnium and neodymium isotopes. *Nature*. 379: 624-627.

Vervoort, J. D., W. M. White, and R. Thorpe, 1994. Nd and Pb isotope ratios of the Abitibi greenstone belt: new evidence for very early differentiation of the Earth. *Earth and Planetary Science Letters,* 128: 215-229.

von Blanckenburg, F., O'Nions, R. K. & Heinz, J. R. 1996. Distribution and sources of pre-anthropogenic lead isotopes in deep ocean water from Fe–Mn crusts. *Geochimica et Cosmochimica Acta*, 60, 4957-4963, doi: 10.1016/S0016-7037(96)00310-9.

Wänke, H., Dreibus, G. & Jagoutz, E. 1984. Mantle geochemistry and accretion history of the earth. In: Kröner, A. (ed.) Archean Geochemistry. Berlin: Springer.

Wedepohl, K. H., 1995. The composition of the continental crust, *Geochimica et Cosmochimica Acta*, 59:1217-1232.

White, W. M., and B. Dupré, Sediment subduction and magma genesis in the Lesser Antilles: isotopic and trace element constraints, *J. Geophys. Res*., 91, 5927-5941, 1986.

White, W. M., Geochemical evidence for crust-to-mantle recycling in subduction zones, in *Crust/Mantle Recycling at Convergence Zones*, vol. edited by S. R. H. a. L. Gulen, 43-58 pp., Kluwer Academic Publishers, Dordrecht, 1989.

White, W. M., P. J. Patchett and D. BenOthman, 1986. Hf isotope ratios of marine sediments and Mn nodules: evidence for a mantle source of Hf in seawater, *Earth and Planetary Science Letters*, 79:46-54.

Willbold, M., Elliott, T. & Moorbath, S. 2011. The tungsten isotopic composition of the Earth/'s mantle before the terminal bombardment. Nature, 477, 195-198, doi: 10.1038/nature10399.

Willbold, M., Mojzsis, S. J. & Elliott, T. 2013. The ε_{182W} isotope composition of the ca. 3920 Ma Acasta Gneiss Complex. Mineralogical Magazine, 77, 2497,

Woodhouse, O. B., Ravizza, G., Kenison Falkner, K., Statham, P. J. & Peucker-Ehrenbrink, B. 1999. Osmium in seawater: vertical profiles of concentration and isotopic composition in the eastern Pacific Ocean. *Earth and Planetary Science Letters*, 173, 223-233, doi: 10.1016/S0012-821X(99)00233-2.

Wu, J., Rember, R., Jin, M., Boyle, E. A. & Flegal, A. R. 2010. Isotopic evidence for the source of lead in the North Pacific abyssal water. *Geochimica et Cosmochimica Acta*, 74, 4629-4638, doi: 10.1016/j.gca.2010.05.017.

Zartman, R. E., and B. R. Doe, Plumbotectonics: The Model, *Tectonophysics, 75*, 135-162, 1981.

Zimmermann, B., Porcelli, D., Frank, M., Andersson, P. S., Baskaran, M., Lee, D.-C. & Halliday, A. N. 2009. Hafnium isotopes in Arctic Ocean water. *Geochimica et Cosmochimica Acta*, 73, 3218-3233, doi: 10.1016/j.gca.2009.02.028.

Zimmermann, B., Porcelli, D., Frank, M., Rickli, J. r., Lee, D.-C. & Halliday, A. N. 2009. The hafnium isotope composition of Pacific Ocean water. *Geochimica et Cosmochimica Acta*, 73, 91-101, doi: 10.1016/j.gca.2008.09.033.

PROBLEMS

1. If we view Indian Ocean water with ε_{Nd} of -6.6 as a simple mixture of Atlantic water with average ε_{Nd} of -11.4 and Pacific water with average ε_{Nd} of -3.9 (which it is not), what are the proportions of Atlantic and Pacific water in the mixture?

2. Suppose a dacitic magma containing 100 ppm Sr and 25 ppm Nd with $^{87}Sr/^{86}Sr = 0.7076$ and $\varepsilon_{Nd} = -2$ mixes with a basaltic magma with 500 ppm Sr and 5 ppm Nd with $^{87}Sr/^{86}Sr = 0.7035$ and $\varepsilon_{Nd} = +6$. Plot, at intervals of 10% addition of the dacitic magma, the Sr and Nd isotopic composition of the mixture. What is the value of r as defined in equation 7.6?

3. If we assume that Sr in seawater ($^{87}Sr/^{86}Sr = 0.70925$) is a mixture of Sr from rivers ($^{87}Sr/^{86}Sr = 0.7119$) and Sr from mid-ocean ridge hydrothermal systems ($^{87}Sr/^{86}Sr = 0.7030$), what is the proportion of mid-ocean ridge derived Sr in seawater?

4. Average continental crust has $^{147}Sm/^{144}Nd$ of 0.112. Assuming that the average age of the crust is 2.2 Ga and that new crust when it forms as a ε_{Nd} of 0 (i.e., derived from a 'chondritic' mantle), what should the average ε_{Nd} of crust be?

5. Assuming the continental crust has $^{147}Sm/^{144}Nd$ of 0.112 and an ε_{Nd} equal to that of the suspended load of rivers of -10.6, what is the τ_{DM} model age of the crust?

6. The observable modern silicate Earth has today has $^{142}Nd/^{144}Nd = 1.141837$. The initial solar system $^{142}Nd/^{144}Nd$ was 0.141437. Assuming the Earth evolved with a constant $^{144}Sm/^{144}Nd$ from this initial value, what would its effective initial (at the formation of the solar system) $^{144}Sm/^{144}Nd$ be?

7. The present $^{142}Nd/^{144}Nd$ of the Nuvvaugittuq amphibolites is 1.141825. Assume that bulk silicate Earth today has $^{142}Nd/^{144}Nd = 1.141837$ and had effective initial you calculated in Problem 6. If the Nuvvaugittuq amphibolites formed from that bulk silicate Earth reservoir 200 million years after the start of the solar system, what must their $^{144}Sm/^{144}Nd$ have been at the time they formed? What would have been the ratio of the $^{144}Sm/^{144}Nd$ to the bulk silicate Earth $^{144}Sm/^{144}Nd$ have been at that time (in other words, how fractionated would the Sm/Nd ratio have been)?

8. The (CI) chondritic concentration of W is 0.09 ppm while that of the bulk silicate Earth is 0.03 ppm. If the late accretionary veneer consisted of CI chondritic material with $\varepsilon_W = -2$ and the silicate had $\varepsilon_W = +0.13$ before addition of this material, what must the mass fraction of this late accretionary veneer have been?